Received: 11 October 2019 | Revised: 4 February 2020 | Accepted: 7 February 2020

DOI: 10.1002/glia.23804

GLIA

WILEY

RESEARCH ARTICLE

Increased oxidative stress, hyperphosphorylation of tau, and dystrophic microglia in the hippocampus of aged *Tupaia belangeri*

Juan D. Rodriguez-Callejas[1] | Eberhard Fuchs[2] | Claudia Perez-Cruz[1]

[1]Pharmacology Department, CINVESTAV-IPN, Mexico City, Mexico

[2]German Primate Center, Leibniz Institute for Primate Research, Göttingen, Germany

Correspondence
Claudia Perez-Cruz, Pharmacology Department, CINVESTAV-IPN, Av. Politécnico Nacional 2508, Col. San Pedro Zacatenco, Gustavo A. Madero, C.P. 07360, Mexico City, Mexico.
Email: cperezc@cinvestav.mx

Funding information
Consejo Nacional de Ciencia y Tecnología, Grant/Award Number: 308515

Abstract

Aging is a major risk factor for the development of neurodegenerative diseases. Alzheimer's disease and other neurodegenerative diseases are characterized by abnormal and prominent protein aggregation in the brain, partially due to deficiency in protein clearance. It has been proposed that alterations in microglia phagocytosis and debris clearance hasten the onset of neurodegeneration. Dystrophic microglia are abundant in aged humans, and it has been associated with the onset of disease. Furthermore, alterations in microglia containing ferritin are associated with neurodegenerative conditions. To further understand the process of microglia dysfunction during the aging process, we used hippocampal sections from *Tupaia belangeri* (tree shrews). Adult (mean age 3.8 years), old (mean age 6 years), and aged (mean age 7.5 years) tree shrews were used for histochemical and immunostaining techniques to determine ferritin and Iba1 positive microglia, iron tissue content, tau hyperphosphorylation and oxidized-RNA in dentate gyrus, subiculum, and CA1-CA3 hippocampal regions. Our results indicated that aged tree shrews presented an increased number of activated microglia containing ferritin, but microglia labeled with Iba1 with a dystrophic phenotype was more abundant in aged individuals. With aging, oxidative damage to RNA (8OHG) increased significantly in all hippocampal regions, while tau hyperphosphorylation (AT100) was enhanced in DG, CA3, and SUB in aged animals. Phagocytic inclusions of 8OHG- and AT100-damaged cells were observed in activated M2 microglia in old and aged animals. These data indicate that aged tree shrew may be a suitable model for translational research to study brain and microglia alterations during the aging process.

KEYWORDS

8OHG, arginase-1, AT100, CA1-CA3, dentate gyrus, IL-10, oligodendrocytes, phagocytic, subiculum

1 | INTRODUCTION

Nowadays, people tend to live longer than before, and globally the proportion of older people is growing at a faster rate than the general population. It is predicted that by 2050 more than 16.5% of the total population will be aged 60 years or older (He, Goodkind, & Kowal, 2016). Aging is associated with the development of chronic neurodegenerative diseases, such as Alzheimer's disease (AD), facing nations worldwide for increased budget expenses in the healthcare system.

During aging, iron accumulates in several brain regions (Cook & Yu, 1998; Massie, Aiello, & Banziger, 1983; Ramos et al., 2014), a condition that has been associated with cognitive decline and neurodegeneration (Bartzokis et al., 1994; Dedman et al., 1992; Penke et al., 2012). Iron is a trace element essential for oxidation–reduction catalysis and bioenergetics, but it also plays a key role in the formation of toxic oxygen radicals that can attack all biological molecules. Specialized molecules for the transport (transferrin) and storage (ferritin) of iron have evolved. Ferritin may prevent intracellular iron from reacting with hydrogen peroxide through Fenton reaction, thus decreasing the production of reactive oxygen species (ROS) (Balla et al., 1992; Cermak et al., 1993; Guan et al., 2017; Lin & Girotti, 1998; Orino et al., 2001; Wang et al., 2011). In the brain, ferritin is heavily expressed in oligodendrocytes and microglia (Cheepsunthorn, Palmer, & Connor, 1998; Connor, Boeshore, Benkovic, & Menzies, 1994; Connor & Menzies, 1995). Microglia are resident macrophages of the central nervous system that provide the first line of defense against any invading pathogen (Tremblay et al., 2011). Upon activation, microglia increase the synthesis of pro-inflammatory and anti-inflammatory cytokines and other molecular mediators, leading to the characterization of two different phenotypes: (a) M1 activation, which is associated with inflammation and (b) M2 activation, involved in the removal of cellular debris and damaging agents by phagocytosis (Cameron & Landreth, 2010; Franco & Fernández-Suárez, 2015; Gordon, 2003; Kabba et al., 2017; Orihuela, McPherson, & Harry, 2016; Tang & Le, 2016). Robust microglia proliferation and activation characterizes AD pathology (Cameron & Landreth, 2010; Floden & Combs, 2011; von Bernhardi, Eugenín-von Bernhardi, & Eugenín, 2015); however, brain iron accumulation does not parallel the increases in ferritin expression in AD patients (Castellani et al., 2004; Lopes, Sparks, & Streit, 2008). Previous reports described that microglia expressing L-chain ferritin shows a dystrophic phenotype in AD and other neurodegenerative diseases (i.e., such as Huntington disease, Down syndrome, dementia with Lewy bodies) (Lopes et al., 2008; Simmons et al., 2007; Streit, Braak, Xue, & Bechmann, 2009; Streit & Xue, 2016; Xue & Streit, 2011). It is postulated that dystrophic microglia loses its function as cytoplasmic disruption occurs (Tischer et al., 2016) resulting in neuronal vulnerability against invading agents or toxic substances.

Understanding the process of microglia function/dysfunction requires the use of a proper animal model that resembles an aging human brain. A recent analysis showed that several microglia genes are expressed differently in humans and mice as a function of age (Galatro et al., 2017) or after activation (Satoh, Kino, Yanaizu, & Saito, 2018), indicating that rodents may not be an ideal animal model to study the functional roles of microglia. Tree shrews (*Tupaia belangeri*) are small body-sized omnivorous mammals belonging to the order Scandentia (Fuchs, 2015); however, recent genome analysis demonstrated a close genetic relationship to primates (Fan et al., 2013). Their natural habitats are tropical forests and plantation areas in Southeast Asia. They have proved to be useful animal models in many instances where a small omnivorous nonrodent species is required for studying fundamental biological functions and disease mechanisms (Cao, Yang, Su, Li, & Chow, 2003; Fuchs & Corbach-Söhle, 2010; Yao, 2017). For aging studies, tree shrews are ideal models as they have a longer life span compared to rodents (7–8 years), but shorter life span than nonhuman primates (Fuchs & Corbach-Söhle, 2010; Keuker, Keijser, Nyakas, Luiten, & Fuchs, 2005). In addition, tree shrews present a high sequence homology with human proteins, more importantly, with AD-related proteins (i.e., abeta, APP, and tau) (Fan et al., 2018; Meyer, Palchaudhuri, Scheinin, & Flügge, 2000; U. Meyer, Kruhøffer, Flügge, & Fuchs, 1998; Palchaudhuri, Hauger, Wille, Fuchs, & Dautzenberg, 1999; Palchaudhuri et al., 1998; Pawlik, Fuchs, Walker, & Levy, 1999). Furthermore, old tree shrews spontaneously develop mild amyloidosis and somatostatin plaque-like structures in several brain regions (Fan et al., 2018; Yamashita, Fuchs, Taira, & Hayashi, 2010; Yamashita, Fuchs, Taira, Yamamoto, & Hayashi, 2012), showing reductions in serotonergic fiber densities in the hippocampus (Keuker et al., 2005) and impairments in working memory (Keuker, de Biurrun, Luiten, & Fuchs, 2004). In this study, we analyzed the brains of adult, old, and aged tree shrews to determine the presence of dystrophic microglia, oxidized RNA, iron tissue content, and tau hyperphosphorylation. In aged subjects, there was an enhanced number of Iba1-labeled dystrophic microglia in all regions analyzed. Ferritin-containing microglia with an activated morphology increased in some hippocampal regions of aged animals. Some activated microglia were labeled with Arginase-1 and IL-10, indicating an M2 phenotype. Oxidative damage to RNA (8OHG) increased in all regions analyzed during the aging process, similar to tau hyperphosphorylation (AT100). Hippocampal regions with less ferritin-containing microglia (i.e., subiculum) presented abundant iron tissue content and the highest AT100 labeling in aged animals. Thus, tree shrews can be considered a valuable translational animal model for studying the process of human brain aging.

2 | METHODS

2.1 | Subjects

Experimentally naive male tree shrews (*T. belangeri*) were obtained from the breeding colony at the German Primate Center (Göttingen, Germany). Animals were housed individually under standard conditions complying with the European Union guidelines for the accommodation and care of animals used for experimental and other scientific purposes (2007/526/EC) on a 12 hr light/dark cycle with ad libitum access to food and water (Fuchs & Corbach-Söhle, 2010). All animal experiments were performed in accordance with the German Animal Welfare Act, which strictly adheres to the European Union guidelines (EU directive 2010/63/EU). Experienced veterinarians and caretakers constantly monitored the animals. The experiments were approved by the Lower Saxony State Office for Consumer Protection and Food Safety (LAVES, Oldenburg, Germany). Animals did not present neurological disorders or other injuries that could cause trauma to the central nervous system.

2.2 | Tissue preparation

Brains of male tree shrews of different ages were used in the current study: four adult (mean age 3.8 years), four old (mean age 6 years), and four aged (mean age 7.5 years) tree shrews were used based on previous reports (Fan et al., 2018; Keuker et al., 2004, 2005; Wu et al., 2019). Animals were anesthetized with an i.p. injection (0.1 ml/100 g body weight) of GM II (ketamine, 50 mg/ml; xylazine 10 mg/ml; atropin 0.1 mg/ml), and after loss of consciousness they received an i.p. injection of ketamine (400 mg/kg body weight). Bodies were transcardially perfused with cold (4°C) saline (0.9% NaCl) for 5 min. Subsequently, for fixation of the brains, cold (4°C) 4% paraformaldehyde (PFA) in 0.1 M phosphate buffer, pH 7.2, was infused for 15 min. The brains were removed and post fixed in fresh 4% PFA at 4°C, where brains were stored until sectioning. Four days before sectioning, tissue was washed with 0.1 M phosphate buffered saline (PBS: 0.15 M NaCl, 2.97 mM Na_2HPO_4-$7H_2O$, 1.06 mM KH_2PO_4; pH 7.4) and immersed in 30% sucrose in PBS at 4°C. Horizontal sections (40 μm) were obtained from hippocampal formation according to Keuker, Rochford, Witter, and Fuchs (2003) and series were prepared every sixth section (at interval of 240 μm) by use of sliding microtome (Leica RM2235). All brain sections were immediately immersed in cryoprotectant solutions, for light microscopy (300 g sucrose [J.T. Baker]; 400 mL 0.1 M PB, and 300 ml ethylene glycol [Sigma], for 1 L) and for immunofluorescence (300 g sucrose; 10 g polyvinyl pyrrolidone [PVP-40, Sigma]; 500 ml of 0.1 M PB and 300 ml ethylene glycol, for 1 L) and stored at −20°C until use in free-floating immunohistochemistry and immunofluorescence protocols.

2.3 | Immunohistochemistry

Dorsal hippocampal sections were permeabilized with 0.2% Triton X100 in PBS (0.2% PBS-triton) for 20 min at room temperature (RT). Sections were washed in PBS and incubated in 0.3% H_2O_2 (in PBS) for 10 min to inactivate endogenous peroxidase activity. The following washing steps were performed three times, 10 min each, in 0.2% PBS-triton at RT. Sections were incubated in 5% bovine serum albumin (BSA; Sigma) in PBS for 15 min (for anti-8OHG) and 3% BSA by 5 min at RT (for AT100, anti Iba1, and anti-Ferritin), in order to block potential nonspecific antibody binding. Subsequently, sections were incubated overnight at 4°C with the primary antibodies: anti-8OHG (a product of RNA oxidation used as an early marker of oxidative stress; Kasai, Kawai, & Li, 2008), AT100 (phosphorylation of tau protein in the residues Thr212 and Ser214; Zheng-Fischhöfer et al., 1998), anti-Iba1 (ionized calcium binding adaptor molecule 1, a widely used marker of microglia; Imai, Ibata, Ito, Ohsawa, & Kohsaka, 1996) and anti-ferritin (iron storage protein highly expressed in microglia; Zhang, Surguladze, Slagle-Webb, Cozzi, & Connor, 2006) (see Supplementary Table S1) diluted in 0.2% PBS-triton at RT. Thereafter, sections were incubated for 2 hr with secondary horseradish peroxidase-conjugated antibodies (see Supplementary Table S1) in 0.2% PBS-triton at RT. Hydrogen peroxide (0.01%) and DAB (0.06%) in 0.2% PBS-triton were used to develop the horseradish peroxidase enzymatic reaction. The enzymatic reaction was stopped with 0.2% PBS-triton, then sections were mounted on glass slides and left to dry overnight. Dry sections were cover slipped with mounting medium Entellan (Merck).

2.4 | Double labeling immunofluorescence

For double labeling immunofluorescence of 8OHG/Iba1, 8OHG/ferritin, AT100/Iba1, AT100/ferritin, and Iba1/ferritin, sections were permeabilized with 0.2% PBS-triton for 20 min at RT. Thereafter, sections were treated with 5% BSA for 15 min at RT, and coincubated overnight at 4°C with primary antibodies (see Supplementary Table S1). Then, sections were washed with 0.2% PBS-triton, and incubated 2 hr with secondary antibodies (see Supplementary Table S1) diluted in 0.2% PBS-triton at RT. Control sections were processed without the primary antibody. All sections were co-incubated with DAPI (Invitrogen, 1:1,000) in 0.2% PBS-triton for 30 min at RT. The sections were then washed and mounted on glass slides. Dry sections were cover slipped with mounting medium VectaShield (Vector Laboratories).

2.5 | Double labeling immunofluorescence using antibody signal enhancer

For double labeling immunofluorescence of anti-Iba or anti-ferritin, CNPase (a marker of oligodendrocytes) and classical markers of macrophage/microglia M2 state IL10 or Arg1 antibodies (Cherry, Olschowka, & O'Banion, 2014, 2015), we used an antibody signal enhancer (ASE) solution (Flores-Maldonado et al., 2020; Rosas-Arellano et al., 2016). Briefly,

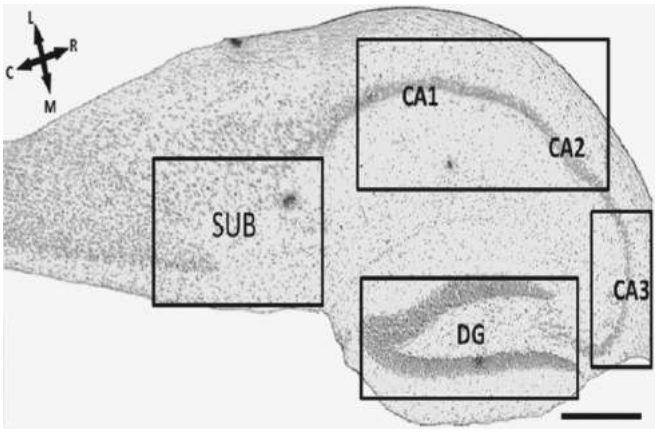

FIGURE 1 Regions of interest through a horizontal section of the hippocampus of the tree shrews. Nissl staining allowed a clear identification of four areas of interest delineated by squares. Subiculum (SUB), CA1-CA3 subfields of the hippocampus (CA1-CA2 and CA3), dentate gyrus (DG). C, caudal; L, left; R, right; R, rostral. (based on Keuker et al. (2003)). Scale bar 100 μm

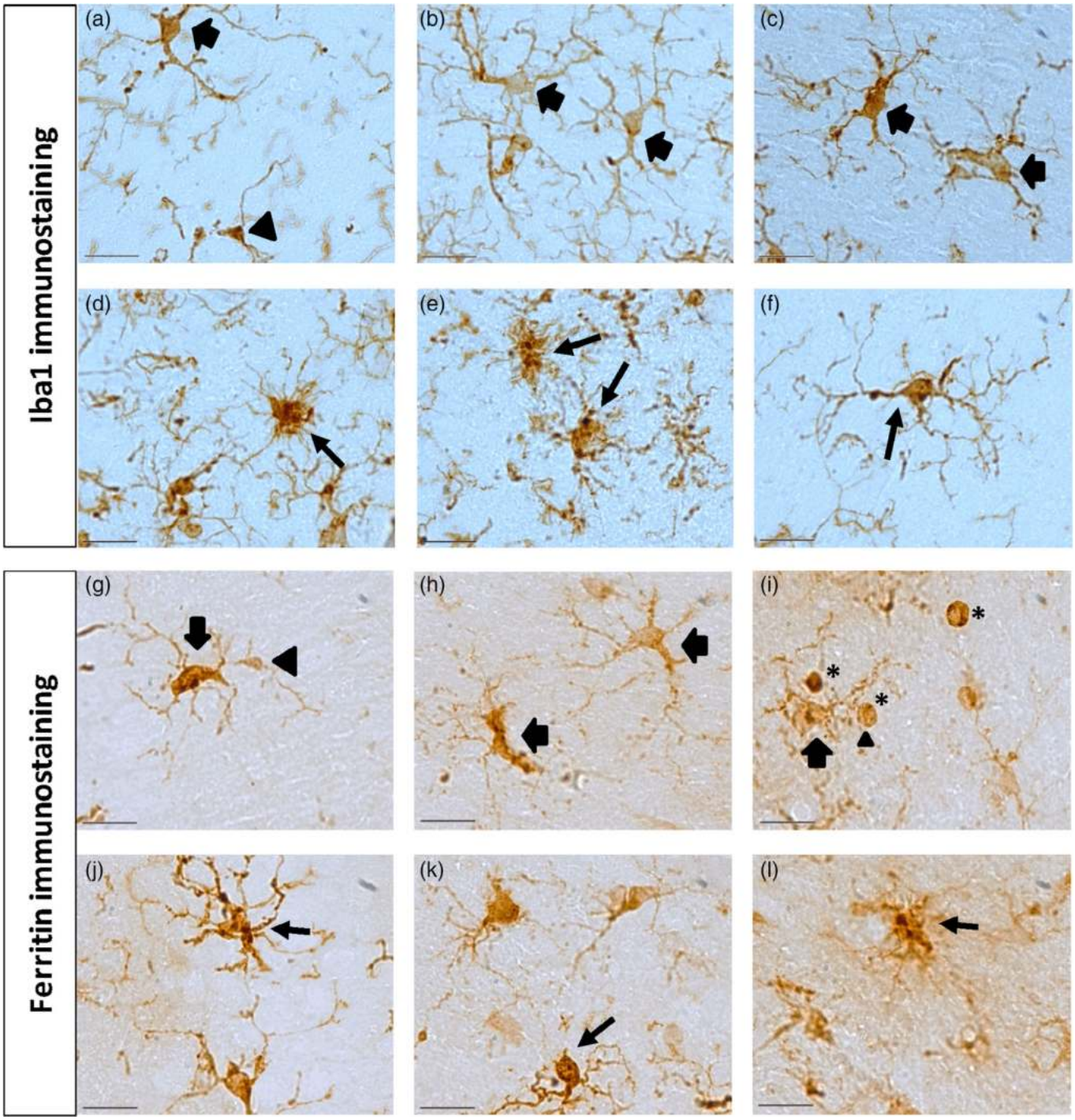

FIGURE 2 Representative photomicrographs of microglia phenotypes using anti-Iba1 or anti-ferritin antibodies. Microglia labeled with Iba1 antibody (a–f) show activated (a–c, thick arrows) and resting phenotype (a, arrowhead). Dystrophic microglia labeled with Iba1 (d–f, thin arrows) showed deramified, short, and tortuous processes. Microglia labeled with ferritin antibody (g–l) showed resting (g, arrowhead) and activated (g–l, thick arrows) phenotypes. Dystrophic microglia labeled with ferritin presented short and deramified processes, spheroids, and cythorrexis (j–l, thin arrows). Note ferritin antibody also labeled oligodendrocytes (i, stars); however, they are clearly distinguishable from microglia due to round soma and absence of process. Scale bar 20 μm [Color figure can be viewed at wileyonlinelibrary.com]

sections were washed with 0.5% PBS-Tween20 twice for 3 min at RT. In order to block potential nonspecific antibody binding, sections were incubated for 30 min using a solution containing 2% donkey serum, 50 mM glycine, 0.05% Tween20, 0.1% TritonX-100, and 0.1% BSA diluted in PBS at RT. For primary antibodies incubation, we used the ASE solution that consisted of 10 mM glycine, 0.05% Tween20, 0.1% TritonX-100, and 0.1% hydrogen peroxide in PBS overnight at 4°C (for antibodies specifications, see Supplementary Table S1). Next day, sections were washed with 0.5% PBS-Tween20 and then were incubated with secondary antibody (see Supplementary Table S1) diluted in 0.1%

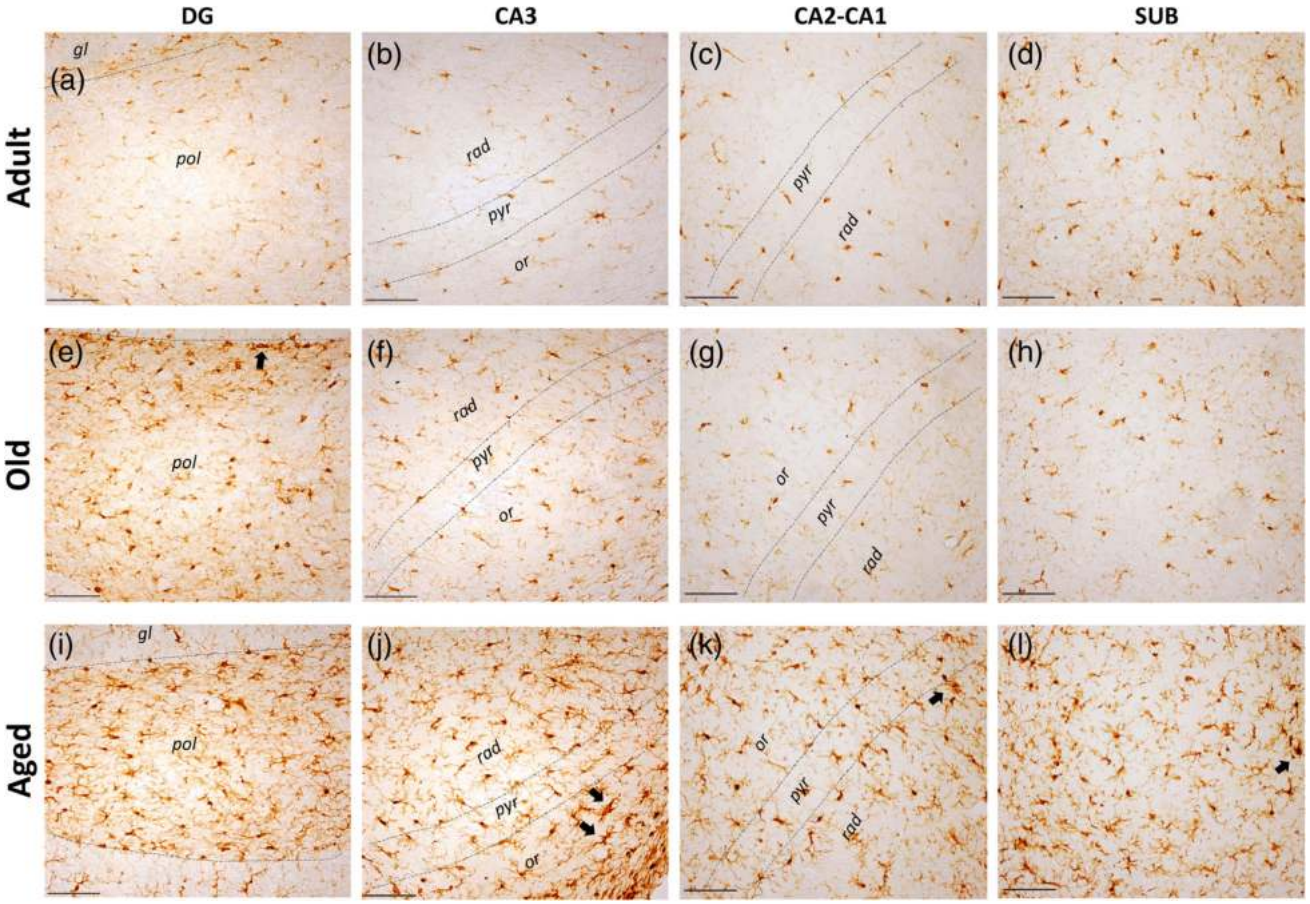

FIGURE 3 Microglia labeled with Iba1 in hippocampus of tree shrews along aging. (a) Iba1-labeled microglia in all regions and ages analyzed. Most Iba1-labeled microglia present a resting and activated morphologies (ah) in adult and old subjects, whereas aged subjects (i–l) showed dystrophic microglia forming clusters with twisted and short processes (arrow). gl, granulare; or, oriens; pol, polymorphic; pyr, piramidale; rad, radiatum. Scale bar 100 μm [Color figure can be viewed at wileyonlinelibrary.com]

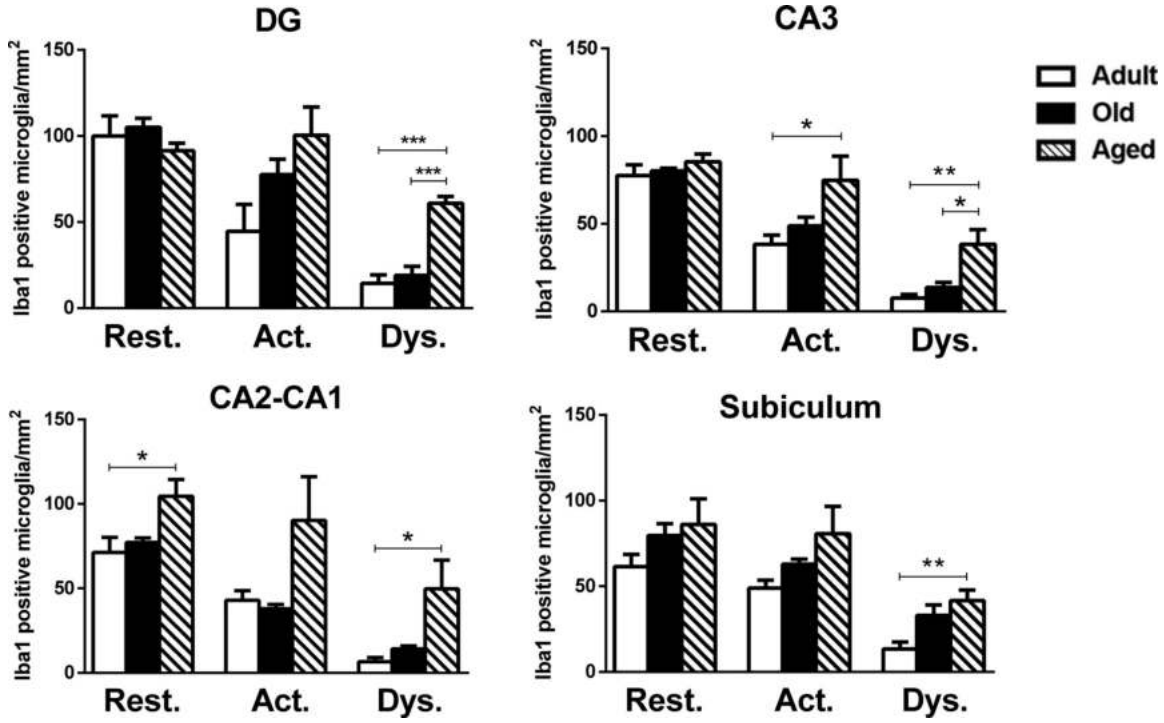

FIGURE 4 Quantification of resting, activated and dystrophic Iba1+microglia per area (mm^2) of tree shrew's hippocampus at different ages. One-way analysis of variance (ANOVA), followed by Tukey's post hoc analysis (*$p < .05$; **$p < .01$; ***$p < .001$)

PBS-Tween20 for 2 hr at RT. Then, sections were rinsed and the standard double labeling immunofluorescence (see Section 2.5) for anti-Iba1 or anti-horse spleen ferritin was followed.

2.6 | Histochemical detection of iron

Detection of iron was performed according to Sands, Leung-Toung, Wang, Connelly, and LeVine (2016). First, slices were incubated in a solution of 1% potassium ferrocyanide trihydrate/5% PVP/0.05 N HCl for 60 min at RT. Sections were washed with water and incubated in methanol containing 0.01 M sodium azide and 0.3% hydrogen peroxide for 75 min at RT. Finally, sections were washed with PBS and incubated in a solution of 10 mg DAB/160 ml 30% H_2O_2/40 ml 0.01 M Tris HCl pH 7.4 for 2 min. Sections were washed, mounted on glass slides and cover slipped with mounting medium Entellan (Merck).

2.7 | Image acquisition

Nikon Eclipse 80i light microscope equipped with a Nikon DS-Ri1 camera was used to acquire bright-field images under 10× (for iron tissue content, AT100 and 8OHG), 20× and 100× (for Iba1 and ferritin) objectives.

For fluorescent labeling, images were obtained by a confocal microscopy Leica TCS-SP8 equipped with Diode (405 nm), OPSL (488 nm), OPSL (552 nm), and diode (638 nm) laser. Both lasers were always used with optimized pinhole diameter and 40×, 65×, and 100× objectives were used. All confocal images were obtained as z-stacks of single optical sections. Stacks of optical sections were superimposed as a single image by using the Leica LASX software.

Hippocampal regions were classified as dentate gyrus (DG), CA3, CA2-CA1, and subiculum (SUB) according to *T. belangeri* neuroanatomical description (Keuker et al., 2003) (Figure 1). For each immunohistochemical/immunofluorescence protocol, at least two or three images from each brain section were used to cover the complete region of interest (see Section 2.8 for details).

2.8 | Morphometry

Microglia quantification and classification were assessed in Iba1 and ferritin positive microglia/oligodendrocytes as described: three images from DG, three images from CA3, three images from CA2-CA1 areas,

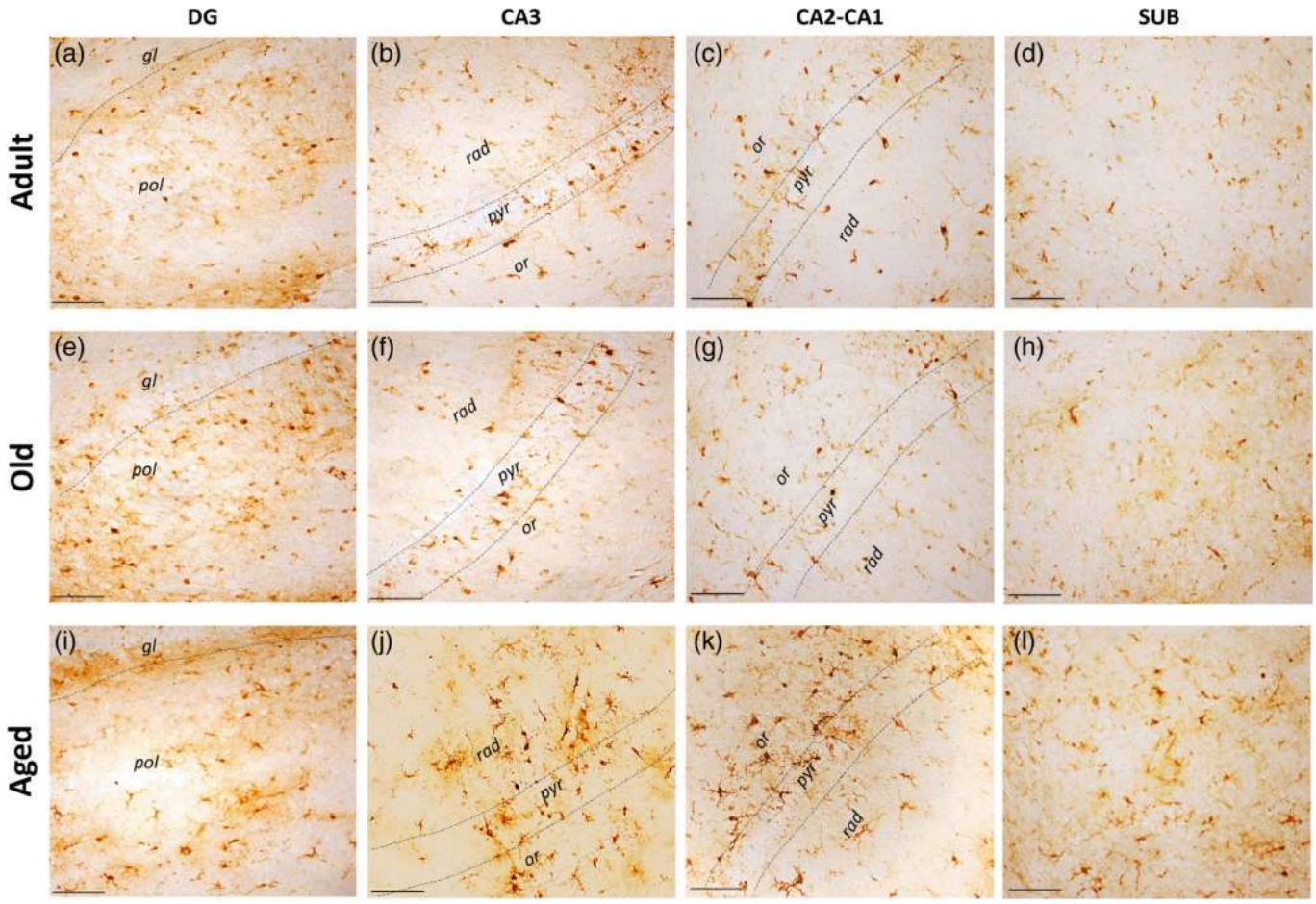

FIGURE 5 Microglia labeled with ferritin in hippocampus of tree shrews along aging. Ferritin-labeled microglia is detected in all regions and ages analyzed. In adults (a–d) and old tree shrews (e–h) ferritin-labeled microglia showed mostly an activated and resting morphology. In aged tree shrews (i–l), predominates the presence of activated microglia. gl, granulare; or, oriens; pol, polymorphic; pyr, piramidale; rad, radiatum. Scale bar 100 μm [Color figure can be viewed at wileyonlinelibrary.com]

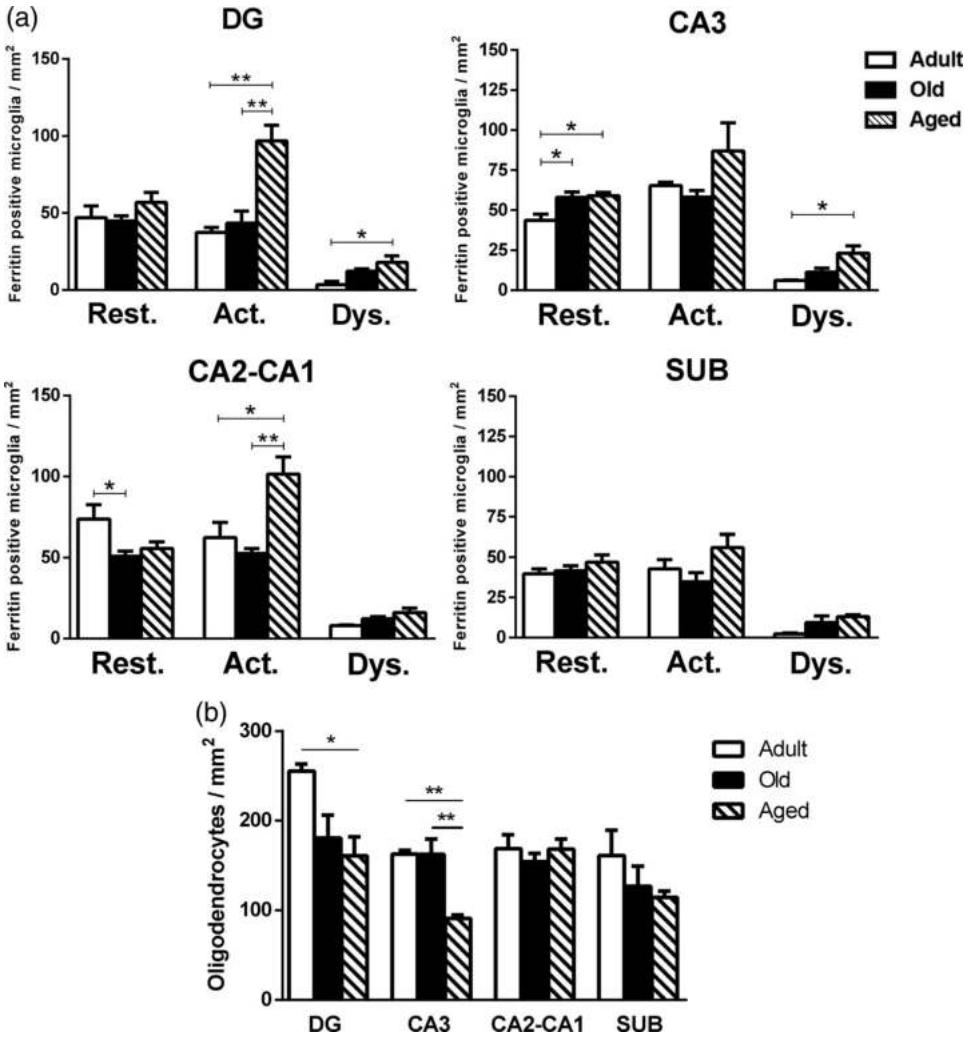

FIGURE 6 Quantification of microglia (a) and oligodendrocytes (b) labeled with ferritin in hippocampus of tree shrews along aging. Resting, activated and dystrophic microglia, or oligodendrocytes were counted per area (mm^2) in the dentate gyrus (DG), CA2, CA2-CA1, and subiculum (SUB) of tree shrew at different ages (adult, old, and aged). One-way analysis of variance (ANOVA), followed by Tukey's post hoc test (*p < .05; **p < .01)

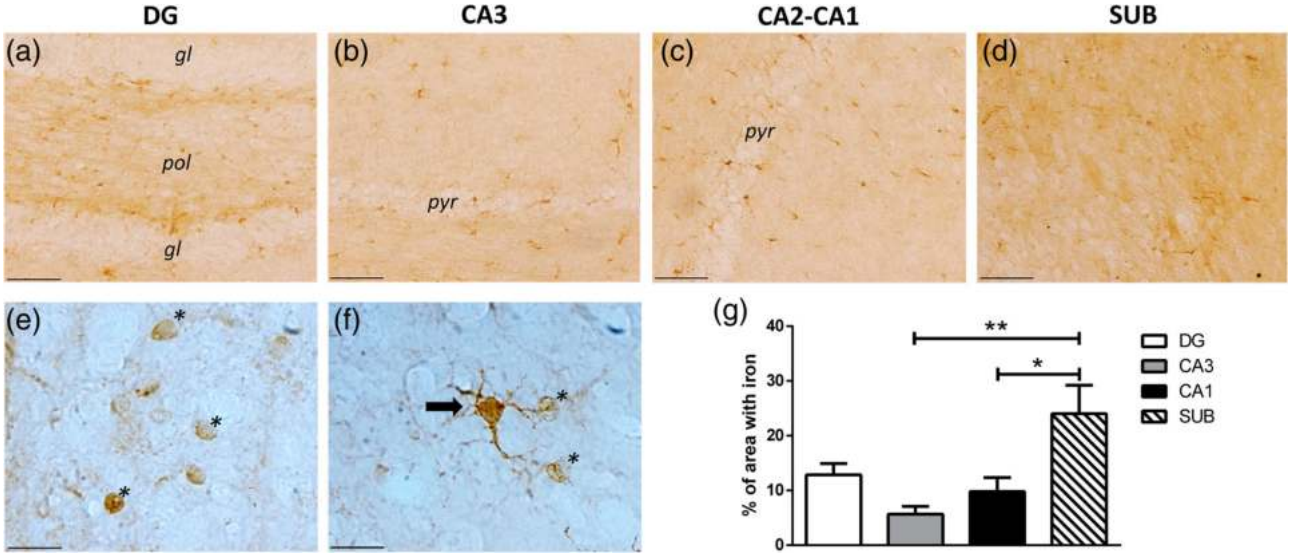

FIGURE 7 Histochemical detection of iron in the tree shrew's hippocampus. Histochemical detection of iron in old and aged tree shrews' hippocampus. Potassium ferrocyanide trihydrate was used to reveal iron content in brain tissue of old and aged tree shrew. The region with highest iron levels was SUB (d and g). As expected, oligodendrocytes-like cells (*, in e,f) and microglia-like cells (arrow, in f) show high levels of iron due to the presence of ferritin. (g) Quantification of area stained with iron showed SUB had the highest iron content compared to other hippocampal regions. DG, dentate gyrus; cornu ammonis (CA) hippocampal regions, CA3 and CA2-CA1; SUB: subiculum. Scale bar 100 μm [Color figure can be viewed at wileyonlinelibrary.com]

and two images from SUB from three brain section per animal from each age group were used. Based on previous descriptions (Rodriguez-Callejas et al., 2019; Rodriguez-Callejas, Fuchs, & Perez-Cruz, 2016; Streit et al., 2009; Streit, Sammons, Kuhns, & Sparks, 2004), cellular morphological characteristics were classified as: resting (displaying a slight ramified morphology and small rounded soma), activated (hypertrophic soma and ramified cells with extensively thick and branched processes), and dystrophic cells (loss of fine branches, presence of shortened tortuous processes and/or cytoplasmic fragmentation). The number of ferritin positive oligodendrocytes was also quantified in same brain sections. Ferritin positive oligodendrocytes were clearly distinguished from microglia due to their circular cytoplasm and the presence of only one or two short processes (Lopes et al., 2008; Rodriguez-Callejas et al., 2019) (Figure 2 and

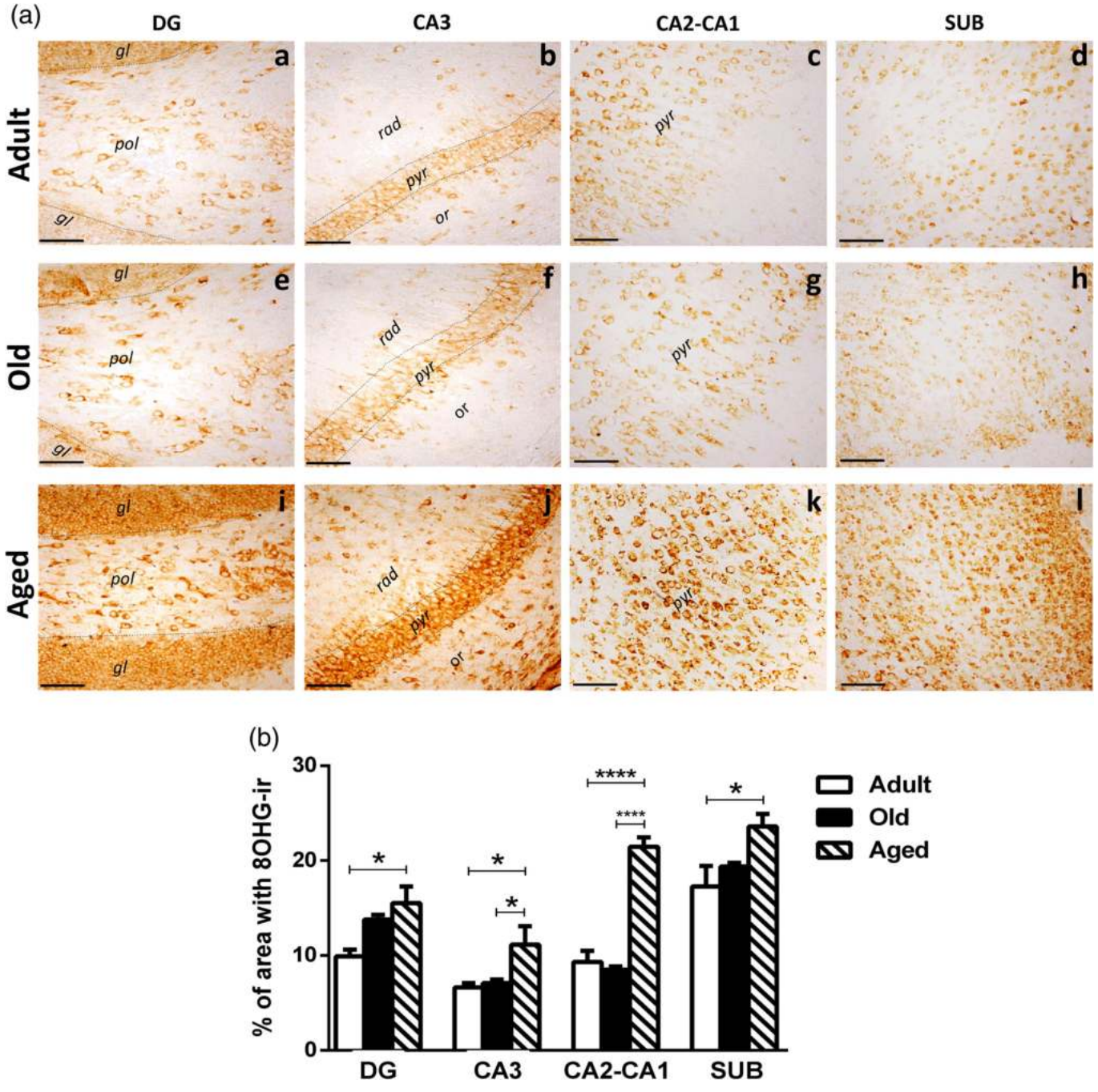

FIGURE 8 Oxidative damage to RNA in hippocampus of tree shrews at different ages. (a) 8-Hydroxiguanosine (8OHG) was used to evaluate damage to RNA due to oxidative stress. Adult (a–d) and old (e–h) tree shrews present a faint 8OHG labeling compared to aged animals (i–l). (b) Percentage of area stained by 8OHG in hippocampus of tree shrew at different ages. DG, dentate gyrus; cornu ammonis (CA) hippocampal regions, CA3 and CA2-CA1; SUB, subiculum. One-way analysis of variance (ANOVA) followed by Tukey's post hoc analysis (*$p < .05$; **$p < .01$; ***$p < .001$; ****$p < .0001$). Scale bar 100 μm [Color figure can be viewed at wileyonlinelibrary.com]

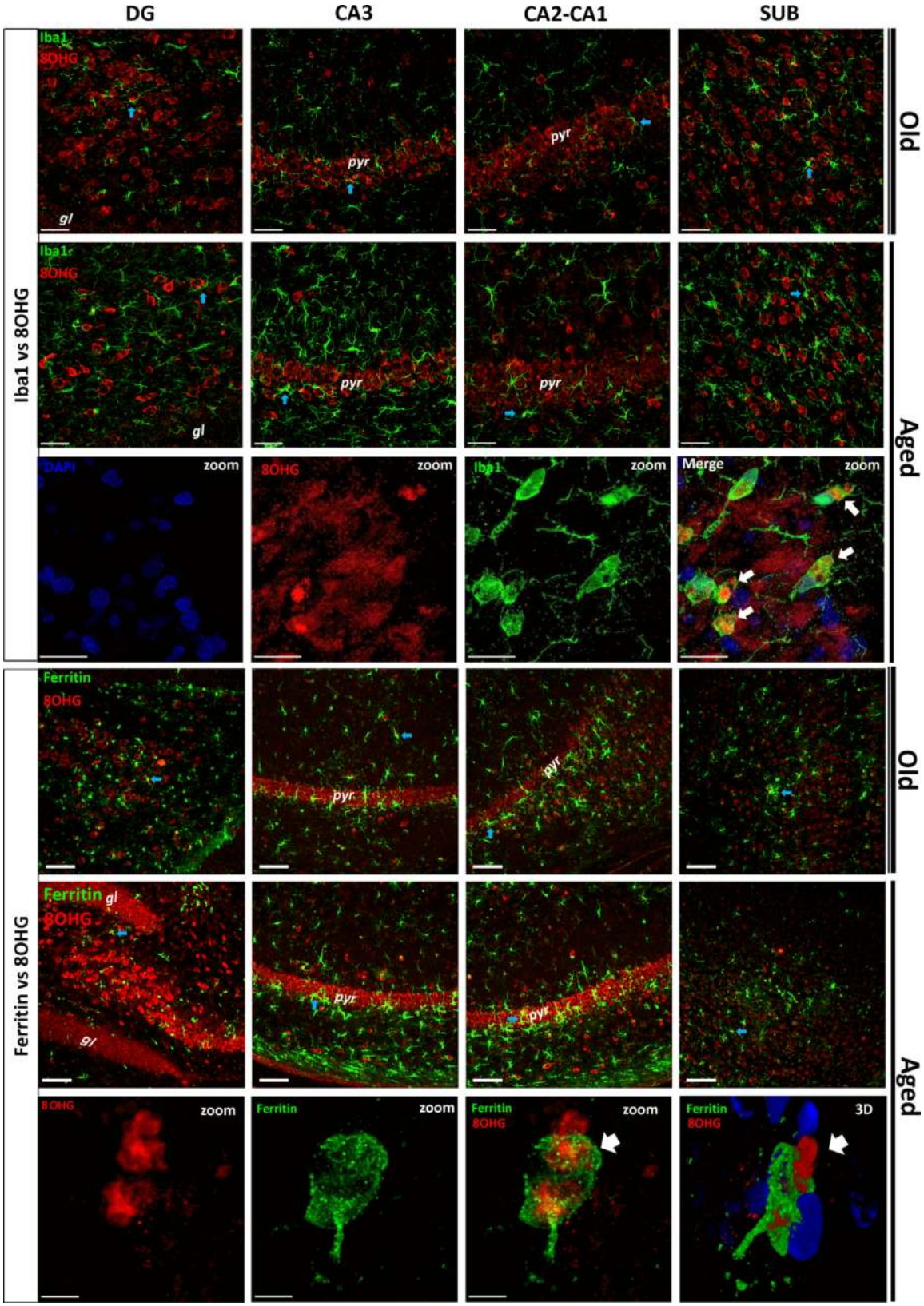

FIGURE 9 Double labeling of microglia (Iba1/ferritin, green) and 8OHG (red) in different hippocampal regions of old and aged tree shrews. Upper panels: Abundant Iba1 positive cells are labeled in hippocampus of old and aged tree shrews. Intense 8OHG staining was observed in principal cells layers (pyr, pyramidal layer, gl, granular layer). Zoom: double-labeled microglia (green) with 8OHG (red) in CA1 region. 3D: Three-dimensional reconstruction and surface rendered z-stack images. Blue arrows: microglia (either Iba1+ or ferritin+) surrounding 8OHG damaged cells. White arrows: activated-like microglia with 8OHG cytoplasmic inclusions. DG, dentate gyrus; cornu ammonis (CA) hippocampal regions, CA3 and CA2-CA1; SUB, subiculum. Scale bar 100 μm, except zoom images (Iba1, scale bar 20 μm; ferritin, scale bar 5 μm) [Color figure can be viewed at wileyonlinelibrary.com]

Supplementary Figure S1b,c). The number of ferritin positive cells (microglia or oligodendrocytes) per unit area (number of cells/ number of images x single image area 0.276 mm^2) was scored in each slice.

To quantify the immunoreactivity (–ir) against AT100 and 8OHG, and iron reactivity we used three brain slices per subject. From each slice, we obtained the following images: two images from DG, three images from CA3, two images from CA2-CA1, and one image from SUB. The total area covered from each region was calculated as the total number of images multiplied by 1,105,440 μm^2 (area of a single image). We used ImageJ software (NIH, Bethesda, MD) to determine the area covered by iron or AT100-ir/8OHG-ir cells. To determine the percentage of immunoreactivity in a determined region, the sum of the areas covered by AT100-ir/8OHG-ir/iron were divided by the total area, and then, multiplied by 100.

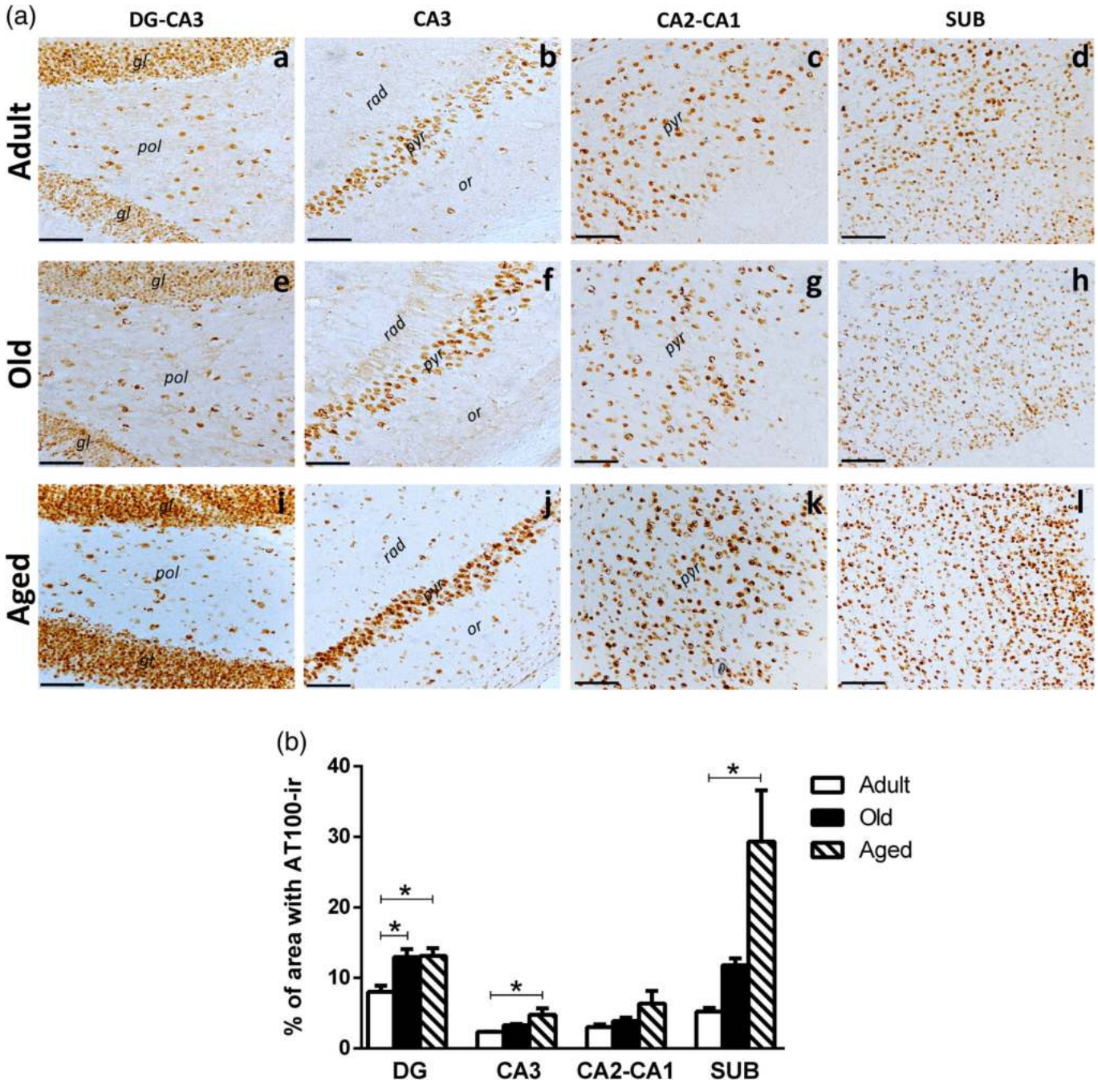

FIGURE 10 Tau phosphorylation in the tree shrew hippocampus increased with aging. (a) Nuclear AT100 labeling increased with aging in different hippocampal regions of tree shrews. AT100 was more abundant in principal cell layers (i.e., pyr: pyramidal layer; gl: granulare layer). Adult (a–d), old (e–h), and aged (i–l) tree shrews. (b) Percentage of area occupied by AT100-ir in hippocampus. DG, dentate gyrus; cornu ammonis (CA) hippocampal regions, CA3 and CA2-CA1; SUB, subiculum. One-way analysis of variance (ANOVA) followed by Tukey's post hoc analysis (*$p < .05$). Scale bar 100 μm [Color figure can be viewed at wileyonlinelibrary.com]

2.9 | Statistical analysis

GraphPad Prism 6.0 software was used for all statistical analysis. One-way analysis of variance (ANOVA) was followed by a Tukey's post hoc test. Differences were considered statistically significant when $p \leq .05$. Data are presented as means ± *SEM*.

3 | RESULTS

Horizontal sections containing the dorsal hippocampus of adult, old, and aged tree shrews were used for the analysis. The areas of interest were subiculum (SUB), CA1-CA3 subfields of the hippocampus (CA2-CA1 and CA3), and DG (Figure 1).

Antibodies previously shown to identify the features of resting, activated, or dystrophic microglia were used. Iba1 and ferritin allowed a clear detection of microglia (Rodriguez-Callejas et al., 2016; Rodriguez-Callejas et al., 2019). Our results showed that the number of Iba1+ resting microglia remains quite stable along aging in all regions analyzed, except in CA2-CA1 region where it increased in aged subjects compared to adults ($p < .05$). Activated microglia labeled with Iba1 tend to show an increased in all regions, but it was significantly different only in CA3 region of aged tree shrews compared to adult subjects ($p < .05$). Dystrophic microglia labeled with Iba1 increased in aged tree shrews

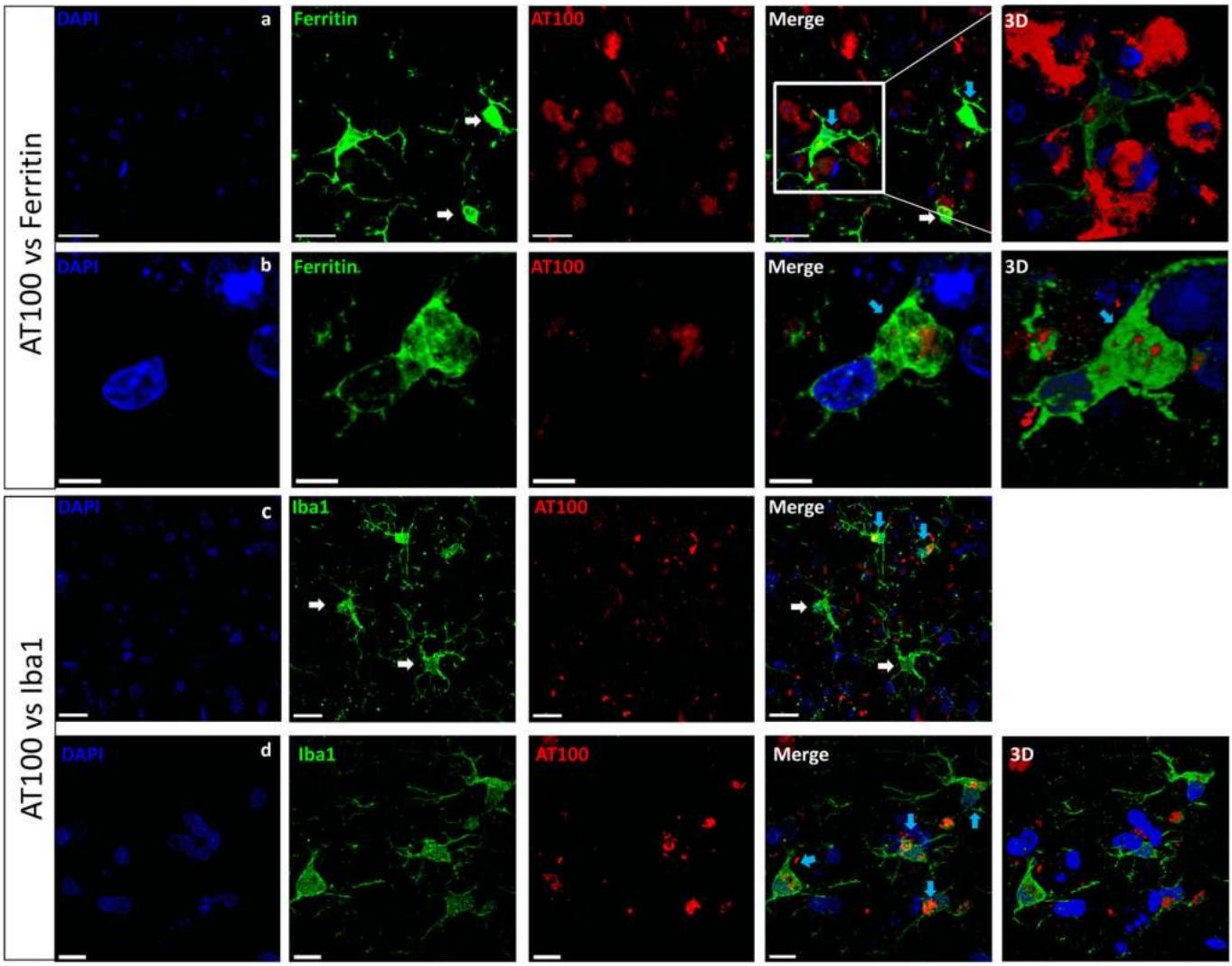

FIGURE 11 Hippocampal microglia presented inclusions of hyperphosphorylated tau in old and aged tree shrews. Upper panels: Double labeling of microglia (ferritin, green) and hyperphosphorylated tau (AT100, red). (a) Representative images from subiculum showed that most microglia's cytoplasm were negative for tau hyperphosphorylation (white arrow), but some activated-like microglia do present AT100 positive staining (blue arrow). Scale bar 20 μm. (b) Representative images from dentate gyrus show active-like microglia with AT100-ir aggregates in the cytoplasmic compartment (blue arrow). Scale bar 5 μm. Lower panels: Double labeling of microglia (Iba1, green) and hyperphosphorylated tau (AT100, red). (c) In CA1, similarly to ferritin-positive microglia, most microglia labeled with Iba1 do not present AT100-ir (white arrows), while few microglia presented cytoplasmic AT100 staining (blue arrows). Scale bar 20 μm. (d) In DG, activated-like microglia presented AT100 staining (blue arrows). Scale bar 10 μm. 3D: Three-dimensional and surface rendering reconstruction [Color figure can be viewed at wileyonlinelibrary.com]

compared to adults and old animals in DG (both $p < .001$) and CA3 ($p < .01$ and $p < .05$, respectively); and in aged compared to old animals in CA2-CA1 ($p < .05$) and SUB ($p < .01$) (Figures 2–4).

Ferritin antibody was used to label microglia and oligodendrocytes. When assessing the number of resting microglia labeled with ferritin, we observed an increase in CA3 of old and aged tree shrews compared to adults (both $p < .05$), but a decrease in CA2-CA1 of adult compared to old animals ($p < .05$). Ferritin+ activated microglia increased in aged tree shrews in all regions analyzed, being significantly different in DG and in CA2-CA1 compared to adult and old animals (DG: both ages, $p < .01$; CA2-CA1, vs. adult $p < .01$, vs. old $p < .05$). Ferritin+ dystrophic microglia showed an increase in DG and CA3 region of aged subjects compared to adult ones (both, $p < .05$) (Figures 5 and 6). Oligodendrocytes labeled with ferritin decreased in aged tree shrews compared to adult and old animals in DG ($p < .05$) and CA3 (both, $p < .01$) (Figures 5 and 6).

In our previous study, iron accumulation in brain tissue was associated with activation of microglia in brain of aged common marmoset. We aimed to determine if iron content will also be increased in aged tree shrews. Iron tissue content was higher in SUB compared to CA3 ($p < .01$) and CA2-CA1 ($p < .05$) in old and aged animals (Figure 7).

Then, we aimed to determine whether iron levels and activation of microglia could be related to oxidative stress damage in brain tissue. 8OHG levels were increased in aged tree shrews in all regions analyzed compared to adults (DG, $p < .05$; CA3, $p < .05$; CA2-CA1, $p < .0001$; SUB $p < .05$) and to old animals (CA3, $p < .05$; CA2-CA1, $p < .0001$) (Figure 8).

RNA oxidation may occur in all cell types (Rodriguez-Callejas et al., 2019). Double labeling of activated microglia either with Iba1 or ferritin and 8OHG allowed us to confirm our previous observation in brain of common marmosets: activated microglia in the hippocampus of tree shrews does not present oxidized-RNA (Figure 9). In general, activated-like microglia (either Iba1+ or ferritin+) were surrounding

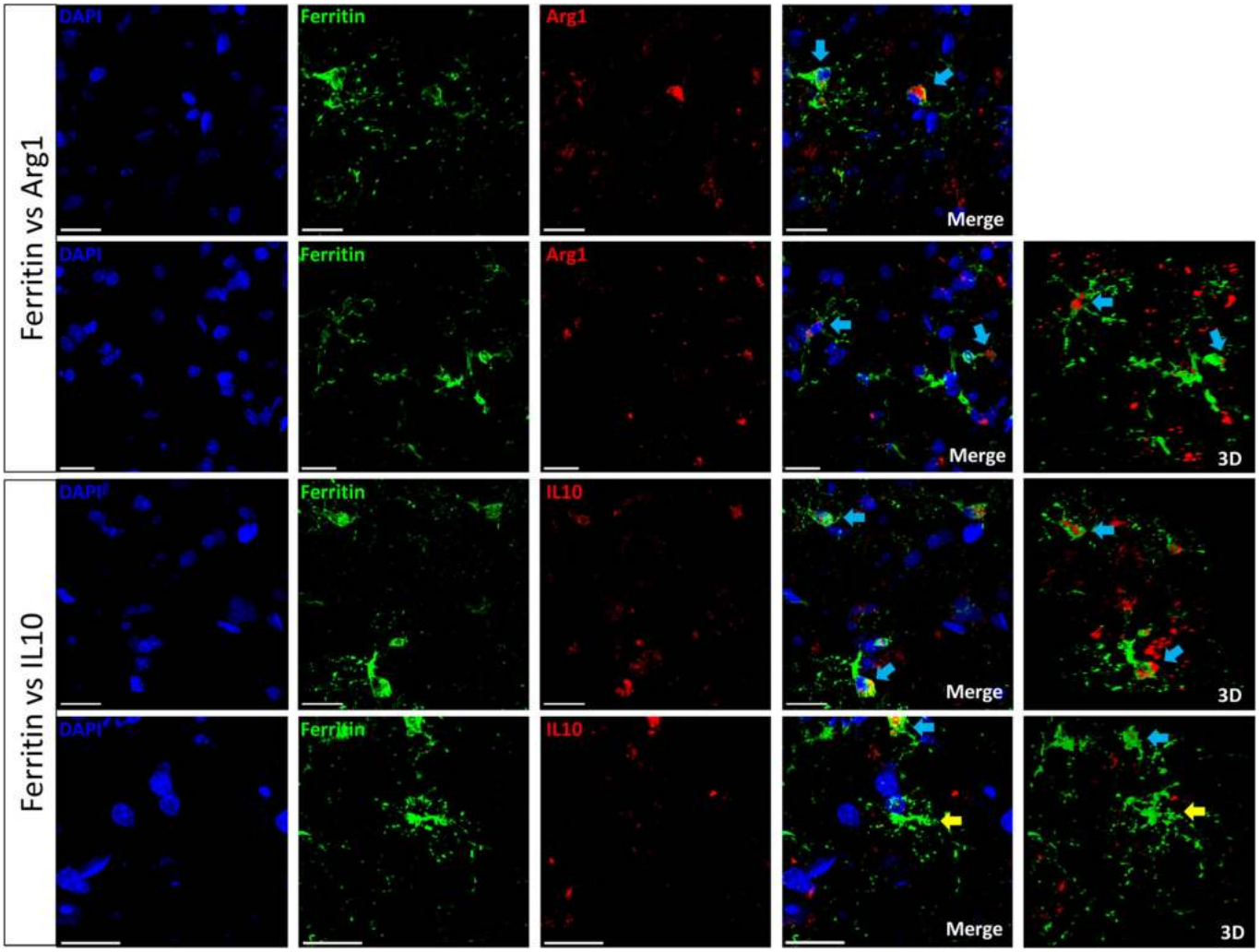

FIGURE 12 Ferritin-labeled microglia showed a phagocytic phenotype. Upper panel: Double labeling of microglia (ferritin, green) and Arginase-1 (Arg1, red). Activated microglia with phagocytic phenotype showed Arg1 staining in cytoplasmic and spheroids compartments (blue arrows). Lower panels: Double labeling of microglia (ferritin, green) and interleukin 10 (IL10, red). Activated microglia with phagocytic phenotype were colabeled with IL10 (blue arrows). Yellow arrow showed a dystrophic microglia (with defragmented cytoplasm and dendritic processes) that did not showed IL10 staining. Scale bar 20 μm [Color figure can be viewed at wileyonlinelibrary.com]

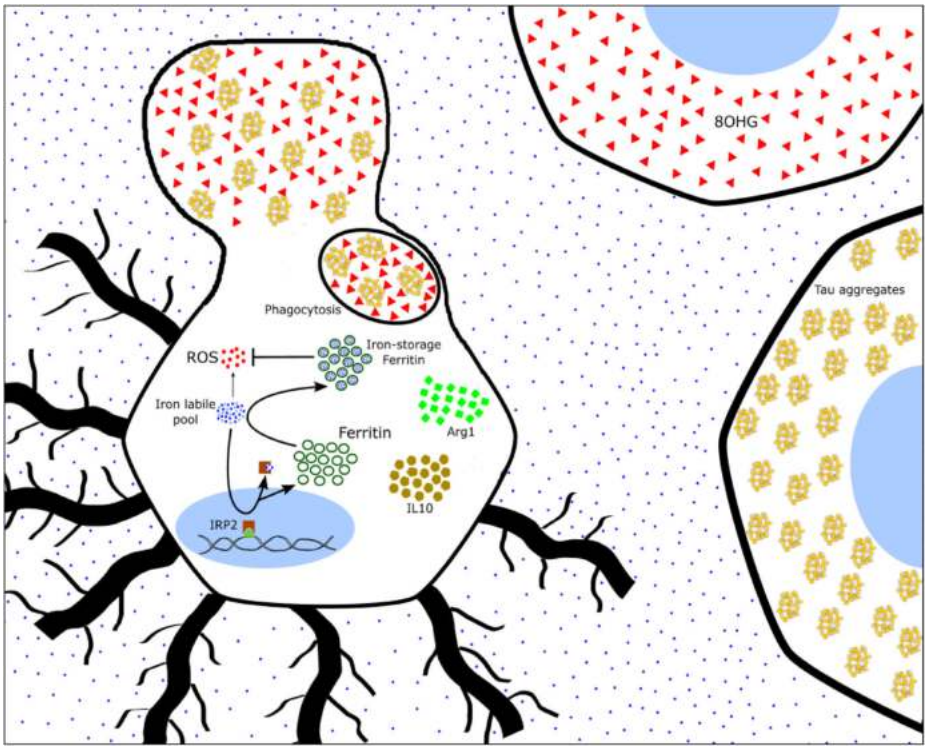

FIGURE 13 Ferritin labeled more activated microglia in aged tree shrews. Activated microglia labeled with Arg1 or IL10 indicates a M2 type. M2 microglia phagocytizes cellular debris or neurons containing high amounts of tau aggregates (AT100) and/or damaged-RNA (8-OHG). Phagocytized material accumulates as cytoplasmic inclusions in old and aged animals [Color figure can be viewed at wileyonlinelibrary.com]

8OHG damaged cells (in pyramidal and granular cell layers). Interestingly, some activated-like microglia presented 8OHG cytoplasmic inclusions, resembling engulfed material. We did not detect whole cytoplasmic 8OHG labeling in microglia, indicating that this 8OHG inclusions may represent phagocytized cellular debris (Figure 9).

We used AT100 to detect tau hyperphosphorylation changes along aging in tree shrews. We detected a nuclear staining with AT100, already since adulthood, in several regions of the hippocampus. However, staining intensity and the amount of nuclear-AT100-ir cells increased with aging, indicating a cumulative process, as observed in aged humans (Gil et al., 2017), common marmosets (Rodriguez-Callejas et al., 2016), and Rhesus monkeys (Härtig et al., 2000). AT100-ir increased in DG, CA3, and SUB of aged tree shrews compared to adults ($p < .05$), and in aged DG compared to old animals ($p < .05$) (Figure 10).

Double labeling of microglia (either with Iba1 or ferritin) and AT100 further corroborates that microglia did not present AT100; however, in hippocampal regions with abundant nuclear-AT100 staining (i.e., *granular* and *polymorphic* layers of the DG, *str. pyramidale* of CA3 and CA2-CA1) some activated-like microglia were AT100+. However, AT100 labeling formed cytoplasmic clusters inside microglia (Figure 11b) similar to the inclusions observed with 8OHG (Figure 9).

Based on these observations, we wanted to determine whether those activated microglia with phagocytic-like inclusion may represent a M2 state. We double-labeled microglia (either with Iba1 or ferritin) with Arg1 or IL10, both classical markers of macrophage/microglia M2 state. We could determine in the hippocampus of aged tree shrews that activated microglia with phagocytic-like features were colabeled with Arg1 or IL10, demonstrating a M2 type (Figure 12).

4 | DISCUSSION

4.1 | Increased amounts of dystrophic microglia labeled with Iba1, and activated microglia labeled with ferritin characterizes the hippocampus of aged tree shrews

We previously described that labeling microglia with both Iba1 and ferritin antibodies allow a clear identification of microglia phenotypes (resting, activated, and dystrophic) in common marmosets (Rodriguez-Callejas et al., 2016; Rodriguez-Callejas et al., 2019). Similarly, in tree shrews, Iba1 and ferritin antibodies were colocalized in the cytoplasmic domain of microglia (Supplementary Figure S1a). However, in agreement with our previous observation in common marmoset (Rodriguez-Callejas et al., 2019), and even though Iba1 labels all microglia or macrophage phenotypes (Imai et al., 1996), in the present study, we observed a higher number of resting (CA2-CA1) and dystrophic (SUB, DG, CA3, CA2-CA1) microglia labeled with Iba1 in the hippocampus of aged tree shrews, while ferritin labeled more activated microglia (DG, CA2-CA1) in aged tree shrews. Furthermore, the number of activated Iba1+ cells was quite homogenous across ages, with a slight increase only in the CA3 region of aged tree shrews compared to younger animals. Previous studies did not show changes in the number of Iba1+ microglia in the hippocampus of aged rats compared to younger animals (VanGuilder et al., 2011). However, it has been reported that microglia proliferation and activation increase in brain specimens of cognitively normal elderly (Conde & Streit, 2006) and AD elderly patients (Cameron & Landreth, 2010; Floden & Combs, 2011; von Bernhardi et al., 2015). Similarly, in the tree shrews, the

total number of Iba1+ cells increased in aged animals compared to old or adult animals in all hippocampal regions analyzed (Supplementary Figure S2).

Ferritin is a heteropolymer formed of two subunits: light chain (L-chain) and heavy chain (H-chain) (Arosio, Ingrassia, & Cavadini, 2009; Chasteen & Harrison, 1999). The proportion of heavy/light subunits depends on the type of cell: neurons mainly express H-rich ferritin (ferroxidase activity), oligodendrocytes express equal amounts of both subunits, while microglia mainly express L-rich ferritin (long-term ferric ion storage) (Cheepsunthorn et al., 1998; Connor et al., 1994; Connor & Menzies, 1995). The ferroxidase activity and long-term iron storage capacity of ferritin results in decreased ROS generation providing important cytoprotectant functions (Balla et al., 1992; Cermak et al., 1993; Guan et al., 2017; Lin & Girotti, 1998; Orino et al., 2001; L. Wang et al., 2011). Ferritin+ microglia with an activated phenotype was increased in aged tree shrews, with the highest amounts in DG, CA2-CA1, and CA3 compared to younger animals. The total number of microglia (resting, activated, and dystrophic) labeled with ferritin increased in aged subjects in all regions analyzed (see Supplementary Figure S2). Thus, tree shrews' microglia suffer similar microglia proliferation as nonhuman primates (common marmoset) and humans (Rodriguez-Callejas et al., 2016; Streit et al., 2004) during aging. Furthermore, activated microglia in hippocampus of old and aged tree shrews were colabeled with Arg1 and IL10, suggesting a phagocytic M2-type. In previous studies, aged common marmosets (mean age 16.83 ± 2.59 years) showed a dramatic reduction in the number of activated ferritin+ microglia, despite significant increases in iron tissue content and 8OHG damage (Rodriguez-Callejas et al., 2019). It was suggested that this decreased number of ferritin-labeled M2 microglia might render the brain of aged common marmosets vulnerable to oxidative stress, a condition that may be linked to the appearance of two main hallmarks of neurodegeneration in these nonhuman primates: amyloid plaques and tau hyperphosphorylation (Rodriguez-Callejas et al., 2016). In the current study, brains of old and aged tree shrews presented activated M2 microglia with phagocytic inclusions. This activated microglia (labeled with ferritin and Iba1) were more abundant in aged animals in almost all regions analyzed, a situation that may suggest an active protective function. Compared to aged marmosets where abundant dystrophic and few activated microglia are observed, in aged tree shrews, the significant abundance of activated microglia in the hippocampus may indicate a still functional and protective role (Figure 13).

Ferritin antibody also allows the quantification of oligodendrocytes. In the tree shrews, we observed a reduction in the number of oligodendrocytes in the hippocampus of aged animals compared to younger animals. The differential expression of ferritin in microglia and oligodendrocytes may reflect cellular-specific ferritin functions/alterations during the process of aging: the increased number of ferritin+ activated microglia may indicate a neuroprotective role in response to the enhanced amount of iron (phagocytosis) as mentioned above; the reduced number of ferritin+ oligodendrocytes may indicate a deficient aging process, as loss of oligodendrocytes and myelin protection has been associated with the course of several neurodegenerative diseases (Jana, Hogan, & Pahan, 2009; Liu & Zhou, 2013).

4.2 | Hyperphosphorylation of tau in the hippocampus of tree shrews

Tau is part of the microtubule-associated protein family whose main function is to facilitate microtubule assembly and stabilization (Butner & Kirschner, 1991). Tau phosphorylation is a process that may be observed under physiological conditions as hibernation (Arendt et al., 2003; Hudson & Scott, 1979), starvation (Yanagisawa, Planel, Ishiguro, & Fujita, 1999) and torpor (Luppi et al., 2019). In aging and neurodegenerative diseases, excessive phosphorylation of tau causes its self-aggregation in straight and paired-helical filaments, which subsequently form the so-called neurofibrillary tangles (NFTs) (Alonso, Zaidi, Novak, Grundke-Iqbal, & Iqbal, 2001; Hof, Glannakopoulos, & Bouras, 1996) resulting in neuronal dysfunction (Ebneth et al., 1998; Stokin & Goldstein, 2006) and eventually neuronal death (Avila, Santa-María, Pérez, Hernández, & Moreno, 2006; Stokin & Goldstein, 2006). Tau hyperphosphorylation and NFT are the main hallmarks of several neurodegenerative diseases, such as AD (Alonso et al., 2001; Braak & Braak, 1991). AT100 labels phosphorylation of residues, Thr212 and Ser214 (Zheng-Fischhöfer et al., 1998), and AT100 localizes in the nucleus of human (Hernández-Ortega, Garcia-Esparcia, Gil, Lucas, & Ferrer, 2016) and mouse (Gärtner, Janke, Holzer, Vanmechelen, & Arendt, 1998) brain samples. Gil et al. (2017) showed that nuclear AT100-ir in human hippocampal neurons increases through aging, reaching the highest levels in senile neurons. However, in AD cases, AT100-nuclear staining progressively decreases with disease severity (Hernández-Ortega et al., 2016) and the staining turns to NFT (Gil et al., 2017). Our present data show an increased nuclear AT100 staining in the hippocampus of aged tree shrews that correlates well with the human aging process.

In nonhuman primates, aging leads to hyperphosphorylated tau filaments formation in neurons, oligodendrocytes and astrocytes (Darusman et al., 2014; Härtig et al., 2000; Oikawa, Kimura, & Yanagisawa, 2010; Perez et al., 2013; Rodriguez-Callejas et al., 2016; Schultz, Dehghani, et al., 2000; Schultz, Hubbard, Rüb, Braak, & Braak, 2000). However, in tree shrews, we did not see AT100-ir in microglia cells, but rather AT100 inclusions. Tau hyperphosphorylation and aggregation are related to iron accumulation; iron accumulates in the brain during normal aging (Ramos et al., 2014; Ward, Zucca, Duyn, Crichton, & Zecca, 2014), mild cognitive impairment (Smith et al., 2010) and AD (Andrasi, Farkas, Scheibler, Reffy, & Bezur, 1995; Smith, Harris, Sayre, & Perry, 1997). Furthermore, iron promotes oxidative damage (Smith et al., 1997) and tau phosphorylation itself (Guo et al., 2013; Xie et al., 2012; Yamamoto et al., 2002). In the present study, SUB was the hippocampal region with the highest amount of AT100 and the highest amount of iron, but the lowest number of ferritin-labeled microglia. This may suggest that the lack of ferritin-positive microglia in SUB may compromise not only iron storage in these cells,

but may promote tau phosphorylation in nearby cells, leaving this brain region highly vulnerable to damage.

4.3 | M2 and dystrophic microglia in old and aged tree shrews

One reliable marker of aging-related oxidative stress is 8OHG, a product of RNA oxidation (Kasai et al., 2008; Syslová et al., 2014). Studies in human, rat and $SOD1^{G93A}$ mice demonstrated that RNA is more vulnerable to oxidative damage than DNA, proteins and lipids (Chang et al., 2008; Fiala, Conaway, & Mathis, 1989; Nunomura et al., 1999). 8OHG increases in liver, kidney, heart, and brain during aging in humans and rodents (Hamilton et al., 2001; Nunomura et al., 2012). Microglia express high amounts of glutathione (Chatterjee, Noack, Possel, Keilhoff, & Wolf, 1999) and glutathione peroxidase (Power & Blumbergs, 2009) that protect from oxidative stress. During microglia activation, the superoxide dismutase 2 (SOD-2) reduces ROS production and contributes to microglia inactivation (resolution of inflammation) (Ishihara, Takemoto, Itoh, Ishida, & Yamazaki, 2015). In addition, the inflammation-related protein autotaxin decreases free radical formation and accumulation of carbonylated proteins (Awada et al., 2012). Overexpression of ferritin may be another factor that protects microglia against oxidative damage during activation (Balla et al., 1992; Cermak et al., 1993; Guan et al., 2017; Lin & Girotti, 1998; Orino et al., 2001; Wang et al., 2011). In the present study, most ferritin+ microglia were not stained with 8OHG, unlike pyramidal neurons and granular cells in old and aged tree shrews that showed an enhanced accumulation of oxidative damage (8OHG) with age.

M1 microglia, called pro-inflammatory microglia, protect tissue against pathogens secreting ROS, reactive nitrogen species (RNS) and several pro-inflammatory cytokines such as IL-β, IL-1α, IL-6, IL-2, TNF-α, CD68, CD32, iNOS, and IFN-γ (Cameron & Landreth, 2010; Orihuela et al., 2016; Tang & Le, 2016). M2 microglia, termed anti-inflammatory microglia, perform the phagocytosis of cell debris, pathogens and misfolded proteins, promote tissue repair, neuron survival and resolution of inflammation (Cameron & Landreth, 2010; Franco & Fernández-Suárez, 2015; Kabba et al., 2017; Orihuela et al., 2016; Tang & Le, 2016). M2 microglia secretes anti-inflammatory cytokines (IL-10, IL-4, IL-13), neurotrophic factors and enhances expression the of arginase-1 (Arg1), FIZZ1 (found in the inflammatory zone), and the chitinase-like protein (Ym1), proteins that promote extracellular matrix repair, and are considered as M2 markers (Cameron & Landreth, 2010; Franco & Fernández-Suárez, 2015; Kabba et al., 2017; Orihuela et al., 2016; Tang & Le, 2016). In this study, we observed that activated microglia were mainly surrounding 8OHG+ cells or presented 8OHG cytoplasmic inclusion. These features have been observed during microglia engulfment of cellular debris, a classical feature of phagocytic M2 activation (Nelson, Warden, & Lenz, 2017; Tichauer & von Bernhardi, 2012; Wang et al., 2013). In previous studies, we also reported amoeboid shaped ferritin+ microglia surrounding 8OHG+ cells. Moreover, those microglia colocalized with Arg1 and IL10 (Rodriguez-Callejas et al., 2019), indicative of M2-activation. Here, we further demonstrate that amoeboid shaped microglia (activated) in the hippocampus of tree shrews were positive for Arg1 and IL10. M2-microglia surrounded AT100+ cells or presented some AT100 inclusions demonstrating a neuroprotective (phagocytic) action (Figure 13). Contrastingly, it has been reported that aged microglia, despite enhancing the expression of genes related to neuroprotection and neurorestoration (Hickman et al., 2013) had a reduced capacity to engulf or clear amyloid-β fibrils (Floden & Combs, 2011). For example, in the visual cortex of old rhesus monkeys, an increased number of intracellular inclusions in microglia has been reported, indicative of increased phagocytosis; however, these microglia showed a reduced capacity to digest the engulfed particles (Peters, Josephson, & Vincent, 1991). This dysfunctional microglia has been related to aging in humans and nonhuman primates (Rodriguez-Callejas et al., 2016; Simmons et al., 2007; Streit et al., 2004; Streit et al., 2009; Verina, Kiihl, Schneider, & Guilarte, 2011; von Eitzen et al., 1998; Xue & Streit, 2011), as it shows deficiencies in the capacity to internalize and degrade toxic extracellular proteins (Borroni et al., 2014; Griciuc et al., 2013; Guerreiro et al., 2013; Kleinberger et al., 2014). Therefore, it has been proposed that dysfunctional microglia with a reduced neuroprotective function may be related to the onset of neurodegeneration (Flanary & Streit, 2004; Streit, 2006; Streit, Xue, Tischer, & Bechmann, 2014). In the hippocampus of tree shrews, we observed an increased number of dystrophic microglia in DG and CA3 regions. Thus, it is tempting to suggest that after a long-term activation (about 4 years from adulthood to aging), the neuroprotective function of M2 microglia declines due to the accumulation of cellular debris (such as AT100) and oxidative stress, and consequently microglia cells enter into dystrophy.

In conclusion, tree shrews presented age-dependent brain alterations such as iron accumulation, oxidative damage, and microglia activation as described in aged humans (Norden & Godbout, 2013; Ramos et al., 2014; Streit et al., 2004; Syslová et al., 2014) and nonhuman primates (Csiszar et al., 2012; Knauer et al., 2017; Rodriguez-Callejas et al., 2016; Rodriguez-Callejas et al., 2019; Roede et al., 2013; Verina et al., 2011). In addition, their shorter life span, plus the spontaneous development of dystrophic microglia, amyloid beta aggregates and tau hyperphosphorylation, tree shrews are proposed as an excellent animal model for the study of brain aging.

ACKNOWLEDGMENT

J.D.D.R.-C., CONACYT Scholarship no. 308515.

CONFLICT OF INTEREST

The authors declare no conflict of interest.

DATA AVAILABILITY STATEMENT

The data that support the findings of this study are available from the corresponding author upon reasonable request.

ORCID

Claudia Perez-Cruz https://orcid.org/0000-0002-5983-307X

REFERENCES

Alonso, A., Zaidi, T., Novak, M., Grundke-Iqbal, I., & Iqbal, K. (2001). Hyperphosphorylation induces self-assembly of tau into tangles of paired helical filaments/straight filaments. *Proceedings of the National Academy of Sciences of the United States of America*, *98*(12), 6923–6928. https://doi.org/10.1073/pnas.121119298

Andrasi, E., Farkas, E., Scheibler, H., Reffy, A., & Bezur, L. (1995). Al, Zn, Cu, Mn and Fe levels in brain in Alzheimer's disease. *Archives of Gerontology and Geriatrics*, *21*(0167–4943), 89–97. https://doi.org/10.1016/0167-4943(95)00643-Y

Arendt, T., Stieler, J., Strijkstra, A. M., Hut, R. A., Rüdiger, J., Van der Zee, E. A., … Härtig, W. (2003). Reversible paired helical filament-like phosphorylation of tau is an adaptive process associated with neuronal plasticity in hibernating animals. *Journal of Neuroscience*, *23*(18), 6972–6981.

Arosio, P., Ingrassia, R., & Cavadini, P. (2009). Ferritins: A family of molecules for iron storage, antioxidation and more. *Biochimica et Biophysica Acta - General Subjects*, *1790*(7), 589–599. https://doi.org/10.1016/j.bbagen.2008.09.004

Avila, J., Santa-María, I., Pérez, M., Hernández, F., & Moreno, F. (2006). Tau phosphorylation, aggregation, and cell toxicity. *Journal of Biomedicine and Biotechnology*, *2006*, 1–5. https://doi.org/10.1155/JBB/2006/74539

Awada, R., Rondeau, P., Grès, S., Saulnier-Blache, J. S., Lefebvre D'Hellencourt, C., & Bourdon, E. (2012). Autotaxin protects microglial cells against oxidative stress. *Free Radical Biology and Medicine*, *52*(2), 516–526. https://doi.org/10.1016/j.freeradbiomed.2011.11.014

Balla, G., Jacob, H. S., Balla, J., Rosenberg, M., Nath, K., Apple, F., … Vercellotti, G. M. (1992). Ferritin: A cytoprotective antioxidant strategem of endothelium. *Journal of Biological Chemistry*, *267*(25), 18148–18153.

Bartzokis, G., Sultzer, D., Mintz, J., Holt, L., Marx, P., Phelan, C., & Marder, S. (1994). In vivo evaluation of brain iron in Alzheimer's disease and normal subjects using MRI. *Biological Psychiatry*, *35*(7), 480–487. https://doi.org/10.1111/j.1469-8749.2011.03950.x

Borroni, B., Ferrari, F., Galimberti, D., Nacmias, B., Barone, C., Bagnoli, S., … Padovani, A. (2014). Heterozygous TREM2 mutations in frontotemporal dementia. *Neurobiology of Aging*, *35*(4), 934.e7–934.e10. https://doi.org/10.1016/j.neurobiolaging.2013.09.017

Braak, H., & Braak, E. (1991). Neuropathological stageing of Alzheimer-related changes. *Acta Neuropathologica*, *82*, 239–259. https://doi.org/10.1007/BF00308809

Butner, K. A., & Kirschner, M. W. (1991). Tau protein binds to microtubules through a flexible array of distributed weak sites. *The Journal of Cell Biology*, *115*(3), 717–730. https://doi.org/10.1083/jcb.115.3.717

Cameron, B., & Landreth, G. E. (2010). Inflammation, microglia, and Alzheimer's disease. *Neurobiology of Disease*, *37*(3), 503–509. https://doi.org/10.1016/j.nbd.2009.10.006

Cao, J., Yang, E.-B., Su, J.-J., Li, Y., & Chow, P. (2003). The tree shrews: Adjuncts and alternatives to primates as models for biomedical research. *Journal of Medical Primatology*, *32*(3), 123–130. https://doi.org/10.1034/j.1600-0684.2003.00022.x

Castellani, R. J., Honda, K., Zhu, X., Cash, A. D., Nunomura, A., Perry, G., & Smith, M. A. (2004). Contribution of redox-active iron and copper to oxidative damage in Alzheimer disease. *Ageing Research Reviews*, *3*(3), 319–326. https://doi.org/10.1016/j.arr.2004.01.002

Cermak, J., Balla, J., Jacob, H. S., Balla, G., Enright, H., Nath, K., & Vercellotti, G. M. (1993). Tumor cell heme uptake induces ferritin synthesis resulting in altered oxidant sensitivity: Possible role in chemotherapy efficacy. *Cancer Research*, *53*(21), 5308–5313.

Chang, Y., Kong, Q., Shan, X., Tian, G., Ilieva, H., Cleveland, D. W., … Lin, C. L. G. (2008). Messenger RNA oxidation occurs early in disease pathogenesis and promotes motor neuron degeneration in ALS. *PLoS One*, *3*(8), e2849. https://doi.org/10.1371/journal.pone.0002849

Chasteen, N. D., & Harrison, P. M. (1999). Mineralization in ferritin: An efficient means of iron storage. *Journal of Structural Biology*, *126*(3), 182–194. https://doi.org/10.1006/jsbi.1999.4118

Chatterjee, S., Noack, H., Possel, H., Keilhoff, G., & Wolf, G. (1999). Glutathione levels in primary glial cultures: Monochlorobimane provides evidence of cell type-specific distribution. *Glia*, *27*(2), 152–161. https://doi.org/10.1002/(SICI)1098-1136(199908)27:2<152::AID-GLIA5>3.0.CO;2-Q

Cheepsunthorn, P., Palmer, C., & Connor, J. R. (1998). Cellular distribution of ferritin subunits in postnatal rat brain. *Journal of Comparative Neurology*, *400*(1), 73–86. https://doi.org/10.1002/(SICI)1096-9861(19981012)400:1<73::AID-CNE5>3.0.CO;2-Q

Cherry, J. D., Olschowka, J. A., & O'Banion, M. K. (2014). Neuroinflammation and M2 microglia: The good, the bad, and the inflamed. *Journal of Neuroinflammation*, *11*, 1–15. https://doi.org/10.1186/1742-2094-11-98

Cherry, J. D., Olschowka, J. A., & O'Banion, M. K. (2015). Arginase 1+ microglia reduce Aβ plaque deposition during IL-1β-dependent neuroinflammation. *Journal of Neuroinflammation*, *12*(1), 1–13. https://doi.org/10.1186/s12974-015-0411-8

Conde, J. R., & Streit, W. J. (2006). Effect of aging on the microglial response to peripheral nerve injury. *Neurobiology of Aging*, *27*(10), 1451–1461. https://doi.org/10.1016/j.neurobiolaging.2005.07.012

Connor, J. R., Boeshore, K. L., Benkovic, S. A., & Menzies, S. L. (1994). Isoforms of ferritin have a specific cellular distribution in the brain. *Journal of Neuroscience Research*, *37*(4), 461–465. https://doi.org/10.1002/jnr.490370405

Connor, J. R., & Menzies, S. L. (1995). Cellular management of iron in the brain. *Journal of the Neurological Sciences*, *134*(Suppl), 33–44. https://doi.org/10.1016/0022-510X(95)00206-H

Cook, C. I., & Yu, B. P. (1998). Iron accumulation in aging: Modulation by dietary restriction. *Mechanisms of Ageing and Development*, *102*(1), 1–13. https://doi.org/10.1016/S0047-6374(98)00005-0

Csiszar, A., Podlutsky, A., Podlutskaya, N., Sonntag, W. E., Merlin, S. Z., Philipp, E. E. R., … Ungvari, Z. (2012). Testing the oxidative stress hypothesis of aging in primate fibroblasts: Is there a correlation between species longevity and cellular ROS production? *Journals of Gerontology - Series A Biological Sciences and Medical Sciences*, *67*(8), 841–852. https://doi.org/10.1093/gerona/glr216

Darusman, H. S., Gjedde, A., Sajuthi, D., Schapiro, S. J., Kalliokoski, O., Kristianingrum, Y. P., … Hau, J. (2014). Amyloid beta1-42 and the phoshorylated tau threonine 231 in brains of aged Cynomolgus monkeys (*Macaca fascicularis*). *Frontiers in Aging Neuroscience*, *6*, 1–7. https://doi.org/10.3389/fnagi.2014.00313

Dedman, D. J., Treffry, A., Candy, J. M., Taylor, G. A. A., Morris, C. M., Bloxham, C. A., … Harrison, P. M. (1992). Iron and aluminium in relation to brain ferritin in normal individuals and Alzheimer's-disease and chronic renal-dialysis patients. *Biochemical Journal*, *287*(2), 509–514. https://doi.org/10.1042/bj2870509

Ebneth, A., Godemann, R., Stamer, K., Illenberger, S., Trinczek, B., Mandelkow, E. M., & Mandelkow, E. (1998). Overexpression of tau protein inhibits kinesin-dependent trafficking of vesicles, mitochondria, and endoplasmic reticulum: Implications for Alzheimer's disease. *Journal of Cell Biology*, *143*(3), 777–794. https://doi.org/10.1083/jcb.143.3.777

Fan, Y., Huang, Z.-Y., Cao, C.-C., Chen, C.-S., Chen, Y.-X., Fan, D.-D., … Yao, Y.-G. (2013). Genome of the Chinese tree shrew. *Nature Communications*, *4*, 1426. https://doi.org/10.1038/ncomms2416

Fan, Y., Luo, R., Su, L. Y., Xiang, Q., Yu, D., Xu, L., … Yao, Y. G. (2018). Does the genetic feature of the Chinese tree shrew (*Tupaia belangeri chinensis*) support its potential as a viable model for Alzheimer's disease research? *Journal of Alzheimer's Disease*, *61*(3), 1015–1028. https://doi.org/10.3233/JAD-170594

Fiala, E. S., Conaway, C. C., & Mathis, J. E. (1989). Oxidative DNA and RNA damage in the livers of Sprague-Dawley rats treated with the hepatocarcinogen 2-nitropropane. *Cancer Research*, *49*, 5518–5522.

Flanary, B. E., & Streit, W. J. (2004). Progressive telomere shortening occurs in cultured rat microglia, but not astrocytes. *Glia*, *45*(1), 75–88. https://doi.org/10.1002/glia.10301

Floden, A. M., & Combs, C. K. (2011). Microglia demonstrate age-dependent interaction with amyloid-β fibrils. *Journal of Alzheimer's Disease*, *25*(2), 279–293. https://doi.org/10.3233/JAD-2011-101014

Flores-Maldonado, C., Albino-Sánchez, M. E., Rodriguez-Callejas, J. D., Estrada-Mondragon, A., León-Galicia, I., Maqueda-Alfaro, R., … Rosas-Arellano, A. (2020). A low cost antibody signal enhancer improves immunolabeling in cell culture, primate brain and human cancer biopsy. *Neuroscience*. [Epub ahead of print]. https://doi.org/10.1016/j.neuroscience.2020.01.009

Franco, R., & Fernández-Suárez, D. (2015). Alternatively activated microglia and macrophages in the central nervous system. *Progress in Neurobiology*, *131*, 65–86. https://doi.org/10.1016/j.pneurobio.2015.05.003

Fuchs, E. (2015). Tree shrews at the German primate center. *Primate Biology*, *2*(1), 111–118. https://doi.org/10.5194/pb-2-111-2015

Fuchs, E., & Corbach-Söhle, S. (2010). In R. Hubrecht & J. Kirkwood (Eds.), *Tree shrews, in the UFAW handbook on the care and management of laboratory and other research animals* (8th ed.). Oxford, England: Wiley-Blackwell.

Galatro, T. F., Holtman, I. R., Lerario, A. M., Vainchtein, I. D., Brouwer, N., Sola, P. R., … Eggen, B. J. L. (2017). Transcriptomic analysis of purified human cortical microglia reveals age-associated changes. *Nature Neuroscience*, *20*(8), 1162–1171. https://doi.org/10.1038/nn.4597

Gärtner, U., Janke, C., Holzer, M., Vanmechelen, E., & Arendt, T. (1998). Postmortem changes in the phosphorylation state of tau-protein in the rat brain. *Neurobiology of Aging*, *19*(6), 535–543. https://doi.org/10.1016/S0197-4580(98)00094-3

Gil, L., Federico, C., Pinedo, F., Bruno, F., Rebolledo, A. B., Montoya, J. J., … Saccone, S. (2017). Aging dependent effect of nuclear tau. *Brain Research*, *1677*, 129–137. https://doi.org/10.1016/j.brainres.2017.09.030

Gordon, S. (2003). Alternative activation of macrophages. *Nature Reviews Immunology*, *3*(1), 23–35. https://doi.org/10.1038/nri978

Griciuc, A., Serrano-Pozo, A., Parrado, A. R., Lesinski, A. N., Asselin, C. N., Mullin, K., … Tanzi, R. E. (2013). Alzheimer's disease risk gene cd33 inhibits microglial uptake of amyloid beta. *Neuron*, *78*(4), 631–643. https://doi.org/10.1016/j.neuron.2013.04.014

Guan, H., Yang, H., Yang, M., Yanagisawa, D., Bellier, J. P., Mori, M., … Tooyama, I. (2017). Mitochondrial ferritin protects SH-SY5Y cells against H2O2-induced oxidative stress and modulates α-synuclein expression. *Experimental Neurology*, *291*, 51–61. https://doi.org/10.1016/j.expneurol.2017.02.001

Guerreiro, R., Wojtas, A., Bras, J., Carrasquillo, M., Rogaeva, E., Majounie, E., … Hardy, J. (2013). TREM2 variants in Alzheimer's disease. *New England Journal of Medicine*, *368*(2), 117–127. https://doi.org/10.1056/NEJMoa1211851

Guo, C., Wang, P., Zhong, M. L., Wang, T., Huang, X. S., Li, J. Y., & Wang, Z. Y. (2013). Deferoxamine inhibits iron induced hippocampal tau phosphorylation in the Alzheimer transgenic mouse brain. *Neurochemistry International*, *62*(2), 165–172. https://doi.org/10.1016/j.neuint.2012.12.005

Hamilton, M. L., Van Remmen, H., Drake, J. A., Yang, H., Guo, Z. M., Kewitt, K., … Richardson, A. (2001). Does oxidative damage to DNA increase with age? *Proceedings of the National Academy of Sciences of the United States of America*, *98*(18), 10469–10474. https://doi.org/10.1073/pnas.171202698

Härtig, W., Klein, C., Brauer, K., Schüppel, K. F., Arendt, T., Brückner, G., & Bigl, V. (2000). Abnormally phosphorylated protein tau in the cortex of aged individuals of various mammalian orders. *Acta Neuropathologica*, *100*(3), 305–312. https://doi.org/10.1007/s004010000183

He, W., Goodkind, D., & Kowal, P. (2016). An aging world: 2015. International Population Reports. https://doi.org/P95/09-1

Hernández-Ortega, K., Garcia-Esparcia, P., Gil, L., Lucas, J. J., & Ferrer, I. (2016). Altered machinery of protein synthesis in Alzheimer's: From the nucleolus to the ribosome. *Brain Pathology*, *26*(5), 593–605. https://doi.org/10.1111/bpa.12335

Hickman, S. E., Kingery, N. D., Ohsumi, T. K., Borowsky, M. L., Wang, L. C., Means, T. K., & El Khoury, J. (2013). The microglial sensome revealed by direct RNA sequencing. *Nature Neuroscience*, *16*(12), 1896–1905. https://doi.org/10.1038/nn.3554

Hof, P. R., Glannakopoulos, P., & Bouras, C. (1996). The neuropathological changes associated with normal brain aging. *Histology & Histopathology*, *11*(1996), 1075–1088.

Hudson, J. W., & Scott, I. M. (1979). Daily torpor in the laboratory mouse, *Mus musculus* var. Albino. *Physiological Zoology*, *52*(2), 205–218. https://doi.org/10.1086/physzool.52.2.30152564

Imai, Y., Ibata, I., Ito, D., Ohsawa, K., & Kohsaka, S. (1996). A novel gene iba1 in the major histocompatibility complex class III region encoding an EF hand protein expressed in a monocytic lineage. *Biochemical and Biophysical Research Communications*, *224*(3), 855–862. https://doi.org/10.1006/bbrc.1996.1112

Ishihara, Y., Takemoto, T., Itoh, K., Ishida, A., & Yamazaki, T. (2015). Dual role of superoxide dismutase 2 induced in activated microglia: Oxidative stress tolerance and convergence of inflammatory responses. *Journal of Biological Chemistry*, *290*(37), 22805–22817. https://doi.org/10.1074/jbc.M115.659151

Jana, A., Hogan, E. L., & Pahan, K. (2009). Ceramide and neurodegeneration: Susceptibility of neurons and oligodendrocytes to cell damage and death. *Journal of the Neurological Sciences*, *278*(1–2), 5–15. https://doi.org/10.1016/j.jns.2008.12.010

Kabba, J. A., Xu, Y., Christian, H., Ruan, W., Chenai, K., Xiang, Y., … Pang, T. (2017). Microglia: Housekeeper of the central nervous system. *Cellular and Molecular Neurobiology*, *38*, 53–71. https://doi.org/10.1007/s10571-017-0504-2

Kasai, H., Kawai, K., & Li, Y. (2008). Analysis of 8-OH-dG and 8-OH-Gua as biomarkers of oxidative stress. *Genes and Environment*, *30*(2), 33–40. https://doi.org/10.3123/jemsge.30.33

Keuker, J. I. H., de Biurrun, G., Luiten, P. G. M., & Fuchs, E. (2004). Preservation of hippocampal neuron numbers and hippocampal subfield volumes in behaviorally characterized aged tree shrews. *The Journal of Comparative Neurology*, *468*(4), 509–517. https://doi.org/10.1002/cne.10996

Keuker, J. I. H., Keijser, J. N., Nyakas, C., Luiten, P. G. M., & Fuchs, E. (2005). Aging is accompanied by a subfield-specific reduction of serotonergic fibers in the tree shrew hippocampal formation. *Journal of Chemical Neuroanatomy*, *30*(4), 221–229. https://doi.org/10.1016/j.jchemneu.2005.08.005

Keuker, J. I. H., Rochford, C. D. P., Witter, M. P., & Fuchs, E. (2003). A cytoarchitectonic study of the hippocampal formation of the tree shrew (*Tupaia belangeri*). *Journal of Chemical Neuroanatomy*, *26*(1), 1–15. https://doi.org/10.1016/S0891-0618(03)00030-9

Kleinberger, G., Yamanishi, Y., Suárez-Calvet, M., Czirr, E., Lohmann, E., Cuyvers, E., … Haass, C. (2014). TREM2 mutations implicated in neurodegeneration impair cell surface transport and phagocytosis. *Science Translational Medicine*, *6*(243), 1–12. https://doi.org/10.1126/scitranslmed.3009093

Knauer, B., Majka, P., Watkins, K. J., Taylor, A. W. R., Malamanova, D., Paul, B., … Reser, D. H. (2017). Whole-brain metallomic analysis of the common marmoset (*Callithrix jacchus*). *Metallomics*, *9*(4), 411–423. https://doi.org/10.1039/c7mt00012j

Lin, F., & Girotti, A. W. (1998). Hemin-enhanced resistance of human leukemia cells to oxidative killing: Antisense determination of ferritin involvement. *Archives of Biochemistry and Biophysics*, *352*(1), 51–58. https://doi.org/10.1006/abbi.1998.0588

Liu, Y., & Zhou, J. (2013). Oligodendrocytes in neurodegenerative diseases. *Frontiers in Biology*, *8*(2), 127–133. https://doi.org/10.1007/s11515-013-1260-4

Lopes, K. O., Sparks, D. L., & Streit, W. J. (2008). Microglial dystrophy in the aged and Alzheimer's disease brain is associated with ferritin immunoreactivity. *Glia*, *56*(10), 1048–1060. https://doi.org/10.1002/glia.20678

Luppi, M., Hitrec, T., Di Cristoforo, A., Squarcio, F., Stanzani, A., Occhinegro, A., … Cerri, M. (2019). Phosphorylation and dephosphorylation of tau protein during synthetic torpor. *Frontiers in Neuroanatomy*, *13*, 57. https://doi.org/10.3389/fnana.2019.00057

Massie, H. R., Aiello, V. R., & Banziger, V. (1983). Iron accumulation and lipid peroxidation in aging C57BL/6J mice. *Experimental Gerontology*, *18*(4), 277–285. https://doi.org/10.1016/0531-5565(83)90038-4

Meyer, H., Palchaudhuri, M., Scheinin, M., & Flügge, G. (2000). Regulation of α(2A)-adrenoceptor expression by chronic stress in neurons of the brain stem. *Brain Research*, *880*(1–2), 147–158. https://doi.org/10.1016/S0006-8993(00)02787-6

Meyer, U., Kruhøffer, M., Flügge, G., & Fuchs, E. (1998). Cloning of glucocorticoid receptor and mineralocorticoid receptor cDNA and gene expression in the central nervous system of the tree shrew (*Tupaia belangeri*). *Molecular Brain Research*, *55*(2), 243–253. https://doi.org/10.1016/S0169-328X(98)00004-7

Nelson, L. H., Warden, S., & Lenz, K. M. (2017). Sex differences in microglial phagocytosis in the neonatal hippocampus. *Brain, Behavior, and Immunity*, *64*, 11–22. https://doi.org/10.1016/j.bbi.2017.03.010

Norden, D. M., & Godbout, J. P. (2013). Microglia of the aged brain: Primed to be activated and resistant to regulation. *Neuropathology and Applied Neurobiology*, *39*(1), 19–34. https://doi.org/10.1111/j.1365-2990.2012.01306.x

Nunomura, A., Perry, G., Pappolla, M. A., Wade, R., Hirai, K., Chiba, S., & Smith, M. A. (1999). RNA oxidation is a prominent feature of vulnerable neurons in Alzheimer's disease. *The Journal of Neuroscience*, *19*(6), 1959–1964. https://doi.org/10.1523/JNEUROSCI.19-06-01959

Nunomura, A., Tamaoki, T., Motohashi, N., Nakamura, M., McKeel, D. W., Tabaton, M., … Zhu, X. (2012). The earliest stage of cognitive impairment in transition from normal aging to Alzheimer disease is marked by prominent RNA oxidation in vulnerable neurons. *Journal of Neuropathology & Experimental Neurology*, *71*(3), 233–241. https://doi.org/10.1097/NEN.0b013e318248e614

Oikawa, N., Kimura, N., & Yanagisawa, K. (2010). Alzheimer-type tau pathology in advanced aged nonhuman primate brains harboring substantial amyloid deposition. *Brain Research*, *1315*, 137–149. https://doi.org/10.1016/j.brainres.2009.12.005

Orihuela, R., McPherson, C. A., & Harry, G. J. (2016). Microglial M1/M2 polarization and metabolic states. *British Journal of Pharmacology*, *173*(4), 649–665. https://doi.org/10.1111/bph.13139

Orino, K., Lehman, L., Tsuji, Y., Ayaki, H., Torti, S. V., & Torti, F. M. (2001). Ferritin and the response to oxidative stress. *Biochemical Journal*, *357*(1), 241–247. https://doi.org/10.1042/bj3570241

Palchaudhuri, M. R., Hauger, R. L., Wille, S., Fuchs, E., & Dautzenberg, F. M. (1999). Isolation and pharmacological characterization of two functional splice variants of corticotropin-releasing factor type 2 receptor from *Tupaia belangeri*. *Journal of Neuroendocrinology*, *11*(6), 419–428. https://doi.org/https://doi.org/10.1046/j.1365-2826.1999.00348.x

Palchaudhuri, M. R., Wille, S., Mevenkamp, G., Spiess, J., Fuchs, E., & Dautzenberg, F. M. (1998). Corticotropin-releasing factor receptor type 1 from *Tupaia belangeri*. Cloning, functional expression and tissue distribution. *European Journal of Biochemistry/FEBS*, *258*(1), 78–84. https://doi.org/https://doi.org/10.1046/j.1432-1327.1998.2580078.x

Pawlik, M., Fuchs, E., Walker, L. C., & Levy, E. (1999). Primate-like amyloid-β sequence but no cerebral amyloidosis in aged tree shrews. *Neurobiology of Aging*, *20*(1), 47–51. https://doi.org/10.1016/S0197-4580(99)00017-2

Penke, L., Valdés Hernandéz, M. C., Maniega, S. M., Gow, A. J., Murray, C., Starr, J. M., … Wardlaw, J. M. (2012). Brain iron deposits are associated with general cognitive ability and cognitive aging. *Neurobiology of Aging*, *33*(3), 510–517. https://doi.org/10.1016/j.neurobiolaging.2010.04.032

Perez, S. E., Raghanti, M. A., Hof, P. R., Kramer, L., Ikonomovic, M. D., Lacor, P. N., … Mufson, E. J. (2013). Alzheimer's disease pathology in the neocortex and hippocampus of the western lowland gorilla (*Gorilla gorilla* gorilla). *The Journal of Comparative Neurology*, *521*(18), 4318–4338. https://doi.org/10.1002/cne.23428

Peters, A., Josephson, K., & Vincent, S. L. (1991). Effects of aging on the neuroglial cells and pericytes within area 17 of the rhesus monkey cerebral cortex. *The Anatomical Record*, *229*(3), 384–398. https://doi.org/10.1002/ar.1092290311

Power, J. H. T., & Blumbergs, P. C. (2009). Cellular glutathione peroxidase in human brain: Cellular distribution, and its potential role in the degradation of Lewy bodies in Parkinson's disease and dementia with Lewy bodies. *Acta Neuropathologica*, *117*, 63–73. https://doi.org/10.1007/s00401-008-0438-3

Ramos, P., Santos, A., Pinto, N. R., Mendes, R., Magalhães, T., & Almeida, A. (2014). Iron levels in the human brain: A post-mortem study of anatomical region differences and age-related changes. *Journal of Trace Elements in Medicine and Biology*, *28*(1), 13–17. https://doi.org/10.1016/j.jtemb.2013.08.001

Rodriguez-Callejas, J. D., Cuervo-Zanatta, D., Rosas-Arellano, A., Fonta, C., Fuchs, E., & Perez-Cruz, C. (2019). Loss of ferritin-positive microglia relates to increased iron, RNA oxidation, and dystrophic microglia in the brains of aged male marmosets. *American Journal of Primatology*, *81*(2), 1–19. https://doi.org/10.1002/ajp.22956

Rodriguez-Callejas, J. D., Fuchs, E., & Perez-Cruz, C. (2016). Evidence of tau hyperphosphorylation and dystrophic microglia in the common marmoset. *Frontiers in Aging Neuroscience*, *8*(315), 1–15. https://doi.org/10.3389/fnagi.2016.00315

Roede, J. R., Uppal, K., Liang, Y., Promislow, D. E. L., Wachtman, L. M., & Jones, D. P. (2013). Characterization of plasma thiol redox potential in a common marmoset model of aging. *Redox Biology*, *1*(1), 387–393. https://doi.org/10.1016/j.redox.2013.06.003

Rosas-Arellano, A., Villalobos-González, J. B., Palma-Tirado, L., Beltrán, F. A., Cárabez-Trejo, A., Missirlis, F., & Castro, M. A. (2016). A simple solution for antibody signal enhancement in immunofluorescence and triple immunogold assays. *Histochemistry and Cell Biology*, *146*(4), 421–430. https://doi.org/10.1007/s00418-016-1447-2

Sands, S. A., Leung-Toung, R., Wang, Y., Connelly, J., & LeVine, S. M. (2016). Enhanced histochemical detection of iron in paraffin sections of mouse central nervous system tissue: Application in the APP/PS1 mouse model of Alzheimer's disease. *ASN Neuro*, *8*(5), 175909141667097. https://doi.org/10.1177/1759091416670978

Satoh, J. I., Kino, Y., Yanaizu, M., & Saito, Y. (2018). Alzheimer's disease pathology in Nasu-Hakola disease brains. *Intractable and Rare Diseases Research*, *7*(1), 32–36. https://doi.org/10.5582/irdr.2017.01088

Schultz, C., Dehghani, F., Hubbard, G. B., Thal, D. R., Struckhoff, G., Braak, E., & Braak, H. (2000). Filamentous tau pathology in nerve cells, astrocytes, and oligodendrocytes of aged baboons. *Journal of Neuropathology and Experimental Neurology*, *59*(1), 39–52. https://doi.org/10.1093/jnen/59.1.39

Schultz, C., Hubbard, G. B., Rüb, U., Braak, E., & Braak, H. (2000). Age-related progression of tau pathology in brains of baboons. *Neurobiology of Aging*, *21*(6), 905–912. https://doi.org/10.1016/S0197-4580(00)00176-7

Simmons, D. A., Casale, M., Alcon, B., Pham, N. H. A., Narayan, N., & Lynch, G. (2007). Ferritin accumulation in dystrophic microglia is an early event in the development of Huntington's disease. *Glia*, *55*(10), 1074–1084. https://doi.org/10.1002/glia

Smith, M. A., Harris, P. L., Sayre, L. M., & Perry, G. (1997). Iron accumulation in Alzheimer disease is a source of redox-generated free radicals. *Proceedings of the National Academy of Sciences of the United States of America*, *94*(18), 9866–9868. https://doi.org/10.1073/pnas.94.18.9866

Smith, M. A., Zhu, X., Tabaton, M., Liu, G., McKeel, D. W., Cohen, M. L., … Perry, G. (2010). Increased iron and free radical generation in preclinical Alzheimer disease and mild cognitive impairment. *Journal of Alzheimer's Disease*, *19*(1), 353–372. https://doi.org/10.3233/JAD-2010-1239

Stokin, G. B., & Goldstein, L. S. B. (2006). Axonal transport and Alzheimer's disease. *Annual Review of Biochemistry*, *75*(1), 607–627. https://doi.org/10.1146/annurev.biochem.75.103004.142637

Streit, W. J. (2006). Microglial senescence: Does the brain's immune system have an expiration date? *Trends in Neurosciences*, *29*(9), 506–510. https://doi.org/10.1016/j.tins.2006.07.001

Streit, W. J., Braak, H., Xue, Q. S., & Bechmann, I. (2009). Dystrophic (senescent) rather than activated microglial cells are associated with tau pathology and likely precede neurodegeneration in Alzheimer's disease. *Acta Neuropathologica*, *118*(4), 475–485. https://doi.org/10.1007/s00401-009-0556-6

Streit, W. J., Sammons, N. W., Kuhns, A. J., & Sparks, D. L. (2004). Dystrophic microglia in the aging human brain. *Glia*, *45*(2), 208–212. https://doi.org/10.1002/glia.10319

Streit, W. J., & Xue, Q.-S. (2016). Microglia in dementia with Lewy bodies. *Brain, Behavior, and Immunity*, *55*(2016), 191–201. https://doi.org/10.1016/j.bbi.2015.10.012

Streit, W. J., Xue, Q.-S., Tischer, J., & Bechmann, I. (2014). Microglial pathology. *Acta Neuropathologica Communications*, *2*, 142. https://doi.org/10.1186/s40478-014-0142-6

Syslová, K., Böhmová, A., Mikoska, M., Kuzma, M., Pelclová, D., & Kacer, P. (2014). Multimarker screening of oxidative stress in aging. *Oxidative Medicine and Cellular Longevity*, *2014*, 1–14. https://doi.org/10.1155/2014/562860

Tang, Y., & Le, W. (2016). Differential roles of M1 and M2 microglia in neurodegenerative diseases. *Molecular Neurobiology*, *53*(2), 1181–1194. https://doi.org/10.1007/s12035-014-9070-5

Tichauer, J. E., & von Bernhardi, R. (2012). Transforming growth factor-β stimulates β amyloid uptake by microglia through Smad3-dependent mechanisms. *Journal of Neuroscience Research*, *90*(10), 1970–1980. https://doi.org/10.1002/jnr.23082

Tischer, J., Krueger, M., Mueller, W., Staszewski, O., Prinz, M., Streit, W. J., & Bechmann, I. (2016). Inhomogeneous distribution of Iba-1 characterizes microglial pathology in Alzheimer's disease. *Glia*, *64*(9), 1562–1572. https://doi.org/10.1002/glia.23024

Tremblay, M.-E., Stevens, B., Sierra, A., Wake, H., Bessis, A., & Nimmerjahn, A. (2011). The role of microglia in the healthy brain. *Journal of Neuroscience*, *31*(45), 16064–16069. https://doi.org/10.1523/JNEUROSCI.4158-11.2011

VanGuilder, H. D., Bixler, G. V., Brucklacher, R. M., Farley, J. A., Yan, H., Warrington, J. P., … Freeman, W. M. (2011). Concurrent hippocampal induction of MHC II pathway components and glial activation with advanced aging is not correlated with cognitive impairment. *Journal of Neuroinflammation*, *8*, 1–21. https://doi.org/10.1186/1742-2094-8-138

Verina, T., Kiihl, S. F., Schneider, J. S., & Guilarte, T. R. (2011). Manganese exposure induces microglia activation and dystrophy in the substantia nigra of non-human primates. *Neurotoxicology*, *32*(2), 215–226. https://doi.org/10.1016/j.neuro.2010.11.003

von Bernhardi, R., Eugenín-von Bernhardi, L., & Eugenín, J. (2015). Microglial cell dysregulation in brain aging and neurodegeneration. *Frontiers in Aging Neuroscience*, *7*(124), 1–21. https://doi.org/10.3389/fnagi.2015.00124

von Eitzen, U., Egensperger, R., Kösel, S., Grasbon-Fordl, E. M., Imai, Y., Bise, K., … Graeber, M. B. (1998). Microglia and the development of spongiform change in Creutzfeld-Jakob disease. *Journal of Neuropathology and Experimental Neurology*, *57*(3), 246–256. https://doi.org/10.1017/CBO9781107415324.004

Wang, G., Zhang, J., Hu, X., Zhang, L., Mao, L., Jiang, X., … Chen, J. (2013). Microglia/macrophage polarization dynamics in white matter after traumatic brain injury. *Journal of Cerebral Blood Flow and Metabolism*, *33*(12), 1864–1874. https://doi.org/10.1038/jcbfm.2013.146

Wang, L., Yang, H., Zhao, S., Sato, H., Konishi, Y., Beach, T. G., … Tooyama, I. (2011). Expression and localization of mitochondrial ferritin mRNA in Alzheimer's disease cerebral cortex. *PLoS One*, *6*(7), 1–8. https://doi.org/10.1371/journal.pone.0022325

Ward, R. J., Zucca, F. A., Duyn, J. H., Crichton, R. R., & Zecca, L. (2014). The role of iron in brain ageing and neurodegenerative disorders. *The Lancet Neurology*, *13*(10), 1045–1060. https://doi.org/10.1016/S1474-4422(14)70117-6

Wu, Z. C., Gao, J. H., Du, T. F., Tang, D. H., Chen, N. H., Yuan, Y. H., & Ma, K. L. (2019). Alpha-synuclein is highly prone to distribution in the hippocampus and midbrain in tree shrews, and its fibrils seed Lewy body-like pathology in primary neurons. *Experimental Gerontology*, *116* (February 2019), 37–45. https://doi.org/10.1016/j.exger.2018.12.008

Xie, L., Zheng, W., Xin, N., Xie, J. W., Wang, T., & Wang, Z. Y. (2012). Ebselen inhibits iron-induced tau phosphorylation by attenuating DMT1 up-regulation and cellular iron uptake. *Neurochemistry International*, *61*(3), 334–340. https://doi.org/10.1016/j.neuint.2012.05.016

Xue, Q. S., & Streit, W. J. (2011). Microglial pathology in down syndrome. *Acta Neuropathologica*, *122*(4), 455–466. https://doi.org/10.1007/s00401-011-0864-5

Yamamoto, A., Shin, R. W., Hasegawa, K., Naiki, H., Sato, H., Yoshimasu, F., & Kitamoto, T. (2002). Iron (III) induces aggregation of hyperphosphorylated τ and its reduction to iron (II) reverses the aggregation: Implications in the formation of neurofibrillary tangles of Alzheimer's disease. *Journal of Neurochemistry*, *82*(5), 1137–1147. https://doi.org/10.1046/j.1471-4159.2002.01061.x

Yamashita, A., Fuchs, E., Taira, M., & Hayashi, M. (2010). Amyloid beta (Aβ) protein- and amyloid precursor protein (APP)-immunoreactive structures in the brains of aged tree shrews. *Current Aging Science*, *3*(3), 230–238. https://doi.org/BSP/CAS/E-Pub/000015 [pii].

Yamashita, A., Fuchs, E., Taira, M., Yamamoto, T., & Hayashi, M. (2012). Somatostatin-immunoreactive senile plaque-like structures in the frontal cortex and nucleus accumbens of aged tree shrews and Japanese macaques. *Journal of Medical Primatology*, *41*(3), 147–157. https://doi.org/10.1111/j.1600-0684.2012.00540.x

Yanagisawa, M., Planel, E., Ishiguro, K., & Fujita, S. C. (1999). Starvation induces tau hyperphosphorylation in mouse brain: Implications for Alzheimer's disease. *FEBS Letters*, *461*(3), 329–333. https://doi.org/10.1016/S0014-5793(99)01480-5

Yao, Y. G. (2017). Creating animal models, why not use the Chinese tree shrew (*Tupaia belangeri chinensis*)? *Zoological Research*, *38*(3), 118–126. https://doi.org/10.24272/j.issn.2095-8137.2017.032

Zhang, X., Surguladze, N., Slagle-Webb, B., Cozzi, A., & Connor, J. R. (2006). Cellular iron status influences the functional relationship between microglia and oligodendrocytes. *Glia*, *54*(8), 795–804. https://doi.org/10.1002/glia.20416

Zheng-Fischhöfer, Q., Biernat, J., Mandelkow, E. M., Illenberger, S., Godemann, R., & Mandelkow, E. (1998). Sequential phosphorylation of tau by glycogen synthase kinase-3β and protein kinase a at Thr212 and Ser214 generates the Alzheimer-specific epitope of antibody AT100 and requires a paired-helical-filament-like conformation. *European Journal of Biochemistry*, *252*(3), 542–552. https://doi.org/10.1046/j.1432-1327.1998.2520542.x

SUPPORTING INFORMATION

Additional supporting information may be found online in the Supporting Information section at the end of this article.

How to cite this article: Rodriguez-Callejas JD, Fuchs E, Perez-Cruz C. Increased oxidative stress, hyperphosphorylation of tau, and dystrophic microglia in the hippocampus of aged *Tupaia belangeri*. *Glia*. 2020;1–19. https://doi.org/10.1002/glia.23804